NASA CR-144673

PERKIN-ELMER

PERKIN-ELMER
ELECTRO-OPTICAL DIVISION
NORWALK, CONNECTICUT

REPORT NO. 12421

100 CM SOLAR TELESCOPE
PRIMARY MIRROR STUDY

PREPARED FOR

GODDARD SPACE FLIGHT CENTER

GREENBELT, MARYLAND

DATE: MARCH 1975

Ewald Schmidt
NASA Technical Officer

J. H. Oberheuser
Perkin-Elmer Program Manager

REF: 40927

TABLE OF CONTENTS

TABLE OF CONTENTS (Continued)

LIST OF ILLUSTRATIONS

LIST OF TABLES

1.0 INTRODUCTION

The National Aeronautics and Space Administration, Goddard Space Flight Center, intends to develop a Solar Telescope for balloon flights and subsequent Space Shuttle pallet missions. The objective of the study, documented by this report, is to investigate the manufacturing impact of primary mirror configuration on the performance of a 100 cm aperture Solar Telescope.

Three primary mirror configurations were considered: solid, standard lightweight, and mushroom. All of these are of low expansion material.

Specifically, the study consisted of evaluating the mirrors with regard to: Manufacturing Metrology, Manufacturing Risk Factors and Ultimate Quality Assessment. As a result of this evaluation, a performance comparison of the configurations was made. A recommendation of mirror configuration is the final output. These evaluations, comparisons and recommendations are discussed in detail in the following paragraphs.

In addition, three other investigations were completed and are documented in Appendices A through C. Appendix A is a discussion of the accuracy of the analytical methods employed in predicting the self-weight deflection of a mushroom mirror. Appendix B is a recommendation, resulting from this study, for additional Advanced Technology Development studies which would confirm the selection of the recommended primary mirror configuration. Also recommended here are thos studies which would be desirable to further the overall Solar Photcheliograph Program. Appendix C is a discussion of previous work Perkin-Elmer has performed in the design and fabrication of miniscus mirrors.

1.1 BASIC ASSUMPTIONS

As an aid in evaluating the three "given" mirror configurations, a set of basic assumptions was generated and employed throughout the study. They are as follows:

a) The 3 mirror configurations are those given by NASA, Figure 1, (taken from Goddard Drawing #GD1297646, dated 4/1/74).

b) The mirrors are made of CerVit, Low expansion material.

c) The mirror blank supplied by NASA is of good quality (bubble size, etc.). No extraordinary blank preparation is required.

d) The mirrors will have a final aluminum coating with MgF overcoat.

e) The overall finished surface figure error of the mirrors is to be $\lambda/20$ rms wavefront - see paragraph 1.2.

Note: Additional assumptions pertaining to particular evaluations are discussed within pertinent sections of the report.

1.2 PRIMARY MIRROR ERROR BUDGET

An error budget for the three Primary Mirror configurations was generated as a guideline in evaluating the configurations. The main contributors to the budget are: manufacturing errors, gravity release, metrology mount errors, on-orbit thermal distortion, mirror mount constraint forces, and others. Each was assigned a weighting factor based upon Perkin-Elmer's previous experience.

Table 1 contains the resulting error budget. It is based upon an overall $\lambda/20$ rms wavefront error ($\lambda/40$ rms surface quality) for the primary mirror. Previous experience indicates that the budgeted error values are achievable.

Figure 1.

LIGHTWEIGHT VS. MUSHROOM TYPE PRIMARY MIRROR LAYOUT

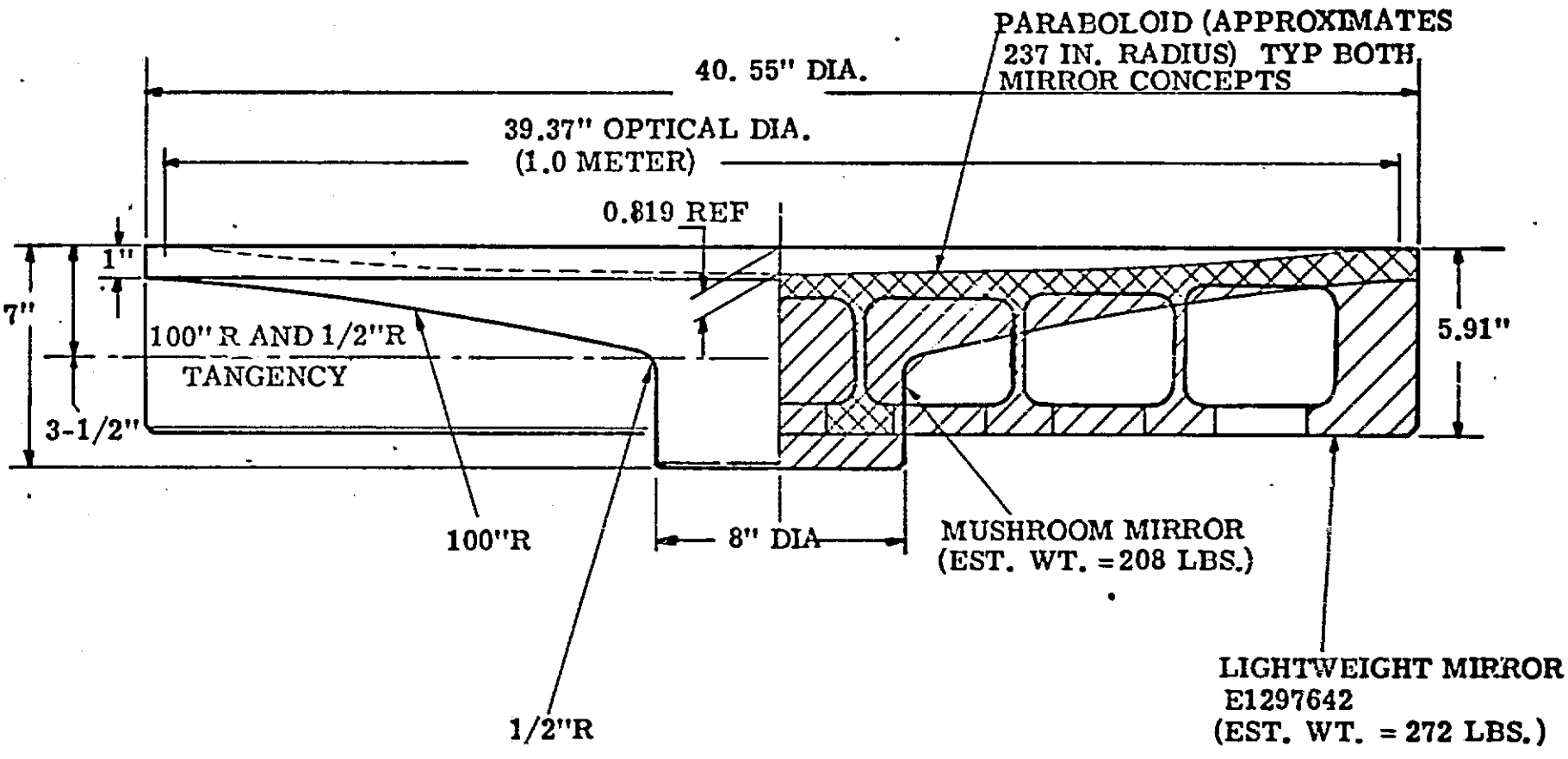

PERKIN-ELMER

Table 1

100 cm PRIMARY MIRROR
ERROR BUDGET

OVERALL ERROR = $\lambda/20$ RMS WAVEFRONT
AT $\lambda = 6323\text{Å} = 25 \times 10^{-6}$ IN

CONTRIBUTORS	RMS WAVEFRONT ERROR
MANUFACTURING	$\lambda/25$
GRAVITY RELEASE	$\lambda/100$
ON-ORBIT THERMAL DISTORTIONS	$\lambda/50$
MOUNT CONSTRAINT FORCES	$\lambda/100$
OTHER ERROR SOURCES	$\lambda/58$
OVERALL; RSS	$\lambda/20 = \lambda/40$ SURFACE

2.0 MANUFACTURING METROLOGY

2.1 MANUFACTURING METROLOGY - SCOPE OF STUDY

In this task the type of metrology mount required for manufacture and test of each of the three mirror configurations was investigated. Reasonable alternatives were also considered. Comparative costs, risk factors, and manufacturing schedule requirements were evaluated.

This task was completed in two steps. Due to the importance of G-release simulation in metrology mount design, a preliminary study of self-weight deflections and the resultant support point requirements was performed first. The results were then employed as a guide in the final mount selection and in the consideration of the remaining variables which impact the mount selection process.

2.2 PRELIMINARY STUDY SIMULATION OF G-RELEASE

The 100 cm Solar Photoheliograph is concepted as an earth orbital solar telescope to be operated under conditions of zero-gravity. The metrology or manufacturing mount for the primary mirror must therefore take this into consideration. It must not only withstand the local loads of grinding and polishing, but also must support the mirror for manufacturing and test in its simulated zero-G shape. It must, point for point, off-load the effects of gravity and self-weight deflection within the limits of the wavefront error budgeted to this source.

The primary mirror error budget allows a $\lambda/100$ rms wavefront error during the simulation of zero-gravity required for manufacturing, testing and operation in a 1-G environment. This implies that in the metrology mounting, the maximum inter-support deformation allowable for the primary mirror under its own weight shall be no greater than $\lambda/200$ rms. The induced telescope wavefront errors are twice the deformations of the mirror.

2.2.1 Self-Weight Deflection

To determine the difficulty in meeting the $\lambda/100$ rms wavefront error requirement, a self-weight deflection analysis was performed on each of the

three primary mirror configurations. The mounting schemes assumed in the analysis are not optimum from a self-weight deflection standpoint. They are those envisioned for the Shuttle flight mounts in a zero-G environment. These schemes tend realistically to yield the largest expected deflection values and thus serve as an indicator of the relative difficulty in meeting the metrology mount corrected self-weight deflection requirements.

The analysis was performed assuming that gravity was acting normal to the front face of the mirror, the attitude normally used in manufacture and manufacturing testing. Both the solid and lightweight configuration were analyzed for three edge support points normal to the face of the mirror. The mushroom configuration has a central hub support.

Table 2 summarized the results. They point out that for 1-G operation all three configurations require a multi-point support for the metrolog mount. All three would also require multi-point support for 1-G teles operation, such as on a Balloon Mission or in ground test.

The table should not be used to make relative comparisons between the three mirror configurations, however, due to the limitations of the approximations used for the mushroom and lightweight configurations. The mushroom mirror, with its inherent tapered shape, required an approximate solution known to yield results of the proper order of magnitude - see Appendix 1. The lightweight mirror, due to its construction, has a considerable amount of inherent shear deflection which was not included in the calculations. Finite-element computer solutions are required on both of these configurations before any accurate comparisons can be made. These limitations, however, do not detract from the usefulness of the results. Orders of magnitude less deflection is required than is predicted for the three mirrors. This indicates the requirements for multi-point metrology mounts.

2.2.2 Simulation of G-Release

An analysis was performed to determine the order of complexity of a metrology mount required to simulate zero-G for manufacturing, testing, and operation in a 1-G environment (balloon flight).

Table 2

PRIMARY MIRROR

SELF-WEIGHT DEFLECTION (IG)

SHUTTLE MISSION MOUNTING SCHEME -

- SOLID – 3 POINT SUPPORT
- CORED, LIGHTWEIGHT – 3 POINT SUPPORT
- MUSHROOM – CENTRAL, HUB MOUNT

PRIMARY MIRROR CONFIGURATION	SELF-WEIGHT DEFLECTION
SOLID	2.095 λ
CORED, LIGHTWEIGHT	3.14 λ
MUSHROOM	8.8 λ

- $\lambda = 6328\text{Å}$
- ALLOWABLE I-G DEFLECTION GRAVITY RELEASE $= \lambda/100$
- ABOVE INDICATES NEED FOR MULTI-POINT MOUNT FOR SUCCESSFUL ONE G OPERATION

The metrology mount envisioned for the three mirrors consists of several support points on the back of the mirror, arranged in a specific, geometric pattern. When subject to a 1-G environment, normal to the front face of the mirror, they will not allow an inter-support deflection greater than the $\lambda/100$ rms wavefront error, budgeted for zero-G simulations.

The analysis performed was intended to generate solely an estimate of the number of support points required for each of the mirror configurations. The analysis was only approximate, as it was based on continuous plate theory and assumed a square array of support points. More accurate results can only be obtained through detailed finite-element computer solutions which must account for the specific geometry of each of the mirror configurations.

Table 3 contains the results of this analysis. They indicate that the mushroom mirror configuration requires substantially more support points than the other two configurations. This implies a greater cost and risk due to the added complexity of the additional support points. This is a negative factor in the final selection between the three mirror configurations.

2.3 RECOMMENDED METROLOGY MOUNT CONCEPT

The Solar Photoheliograph Primary Mirror is required to operate both in a 1-G and zero-G environment corresponding to the Balloon and Shuttle Missions, respectively. Thus, a zero-G simulation required for both the manufacturing and testing phases of the mirror production would encompass both missions of the mirror.

A properly designed metrology mount performs a dual function in that it both supports and positions the primary mirror during both the manufacturing and testing phases of the mirror production process.

In both of these phases the mount must provide zero-gravity simulation - i.e., maximum $\lambda/100$ rms wavefront error between supports - regardless of attitude of the mirror. This is especially important in the Balloon Mission testing phase. Unlike the polishing and grinding phase where the

Table 3

METROLOGY MOUNT
SIMULATION OF G-RELEASE

ALLOWABLE INTERSUPPORT DISPLACEMENT = λ/100 WF RMS AT 6328Å

MIRROR CONFIGURATION	ESTIMATED NUMBER OF SUPPORT POINT REQUIRED*
SOLID	25
LIGHTWEIGHT	25
MUSHROOM	50 → 122

*Approximate analysis based on continuous plate theory and assumed square array of support points.

mirror remains in the horizontal attitude, this testing phase requires that the mirror be tested in many different, non-horizontal attitudes in a 1-G environment to simulate the balloon-borne mission.

Non-horizontal attitudes create components of gravity both normal to and in the plane of the mirror, while the horizontal position of the polishing and grinding phase creates only gravity forces normal to the mirror. Thus, if the metrology mount is to be used only for polishing and grinding, then only simple lateral positioning is required. If variable attitude testing is also required, then lateral gravity support must also be provided. In the Balloon Mission application, lateral positioning and gravity support are required, as well as normal support.

It has been found in Perkin-Elmer's experience, for mirrors of the 100 cm diameter under consideration, that counterweighted metrology mounts provide the best solution to metrology mount requirements.

Counterweights have the advantage of automatically adjusting for attitude changes. They have the additional advantages of being simple, reliable, easily mounted, and can exert a calibrated level of support. They provide both tensile and compressive forces. The number and location of the counterweights, both on the lateral and normal surfaces of the mirror, are determinable through existing analytical techniques for all of the mirror configurations under consideration. They are required to provide the $\lambda/100$ rms wavefront error, for zero-G simulation, for varying mirror attitudes.

The mount contemplated for the solid and lightweighted mirrors, is a multi-point counterweighted one patterned after the Stratoscope 36" primary, manufactured by Perkin-Elmer several years ago. This mount duplicates the mission requirements of the Photoheliograph with respect to its balloon-borne configuration. The mount for the mushroom mirror would be similar but would require a larger number of support points due to its greater flexibility. The Stratoscope design is scaled up to these mirror designs either by addition of support points or increase in scale. As pointed out in the

preliminary zero-G simulation studies, multi-point mounts are required for all three mirror configurations with the number of support points varying for each of the mirror configurations.

The mushroom mirror has a mean thickness of about 2 1/2". This means an aspect ratio of 16 to 1. Considering the mirror to be a plate 2 1/2" thick and supported at three equi-distant points at the 0.7 zone:

$$S = 0.436K \frac{PR^2}{D}$$

where:

P = weight = 234 lbs.

R = radius of the blank = 20"

D = structural rigidity = 18.6×10^6 for CerVit

K = an empirical constant determined by experiment

S = maximum deflection = 4.3 λ @ λ = 5461Å

This self-weight deflection would be quartered by the use of a nine point support to about 1λ. Similar deflections for the solid and light-weighted mirror are 0.7λ and 1.2λ for a three point mount. These deflections necessitate a multi-point mount for manufacturing and testing. It can be inferred that the mushroom would need the maximum number of points and the solid the least. This corroborates the preliminary work done in paragraph 2.2.

Fifty or more points are suggested by the preliminary studies for the mushroom. This implies that this mirror configuration is also quite flexible under externally imposed loads. True support tends to become indeterminate and its achievement risky. The possibility of support point print through, and its subsequent machining into the optical surface, also is greatly increased. The cost of a mount for the mushroom mirror would consequently be higher, due to the need for more in-depth design and analysis time, but the crucial factor is the increased risk in the manufacture of the mirror. Additional load-deflection studies should be done with specific mounting designs for the mirror.

The schedule requirements for each mirror design are fairly straightforward. Once such questions as type of mount and its repeatability are settled, work can be scheduled with confidence. None of the three designs should require special handling as long as the blanks are supplied in their approximate final shape. In particular, if the mushroom mirror must be machined out of a large blank the added tasks must be scheduled to accomplish this. It is assumed this will not be required. Blank bulk machining requirements are not considered in the study.

2.4 ALTERNATE MOUNTING TECHNIQUES

In the above section, only one mount was considered. Three other support methods have been used on mirrors similar to the 100 cm design submitted.

1. One of these methods is an edge mount using a mercury filled ring together with positive air pressure on the back of the mirror. This could be used to support a solid or lightweighted mirror. Experience indicates this mount is difficult to implement effectively. Specifically, the mirror axis must be coincident with that of the "O"-ring seal or the mirror will bind in place. If the "stiction" of the ring material is reduced, the mirror location axially becomes difficult to control. This design was used on a 48" f/2 parabola made at Perkin-Elmer. It required that the mirror be close to horizontal all of the time. Gravity release simulation for multiple attitude testing is not possible and, of course, operation in a vacuum for testing is impossible. Finally, the pressure on the "O"-ring necessary to seal the chamber under pressure has been found to exceed that which would distort the mirror. These reasons, together with the difficulty of operation, make this method one to avoid.

2. A second method of support is one which has been used on miniscus design mirrors, similar to the mushroom mirror, in conjunction with a multi-point support system. Perkin-Elmer has made many

miniscus mirrors, one in particular being the 30" f/0.62 primary for the Super Schmidt Meteor Camera for NASA. Other experience includes 26" solid miniscus mirrors as well as ULE eggcrates. The mounting method involves a variation in design as shown in Figure 2.

The mirror is supported by a ring at the plane of the center of gravity. This design weighs about one-third that of a solid conventional mirror of similar aperture. It should be noted that the thickness of the mirror does not decrease as rapidly as in the NASA design. This gives less self-weight deflection and therefore eases the multi-point support problem.

Variable attitude testing and gravity release simulation are easier to perform with this mount, since the mirror is captured in 5 degrees of freedom.

3. A third mount concept may be considered for this application. Although this mount concept is not backed by experience gained through prior use, the mount has been designed and is being manufactured for use in the manufacture of mirrors for the LST program.

The mount consists of multiple low spring rate supports, arranged in a grid pattern. Each spring support force is adjustable to counter the effect of gravity on the mirror in the vicinity of the support. The spring rate is made low to avoid variation in support force by small normal mirror displacements. Mirror position is controlled by three locating pads on the mirror.

This mount is useful for both mirror manufacture and metrology. It has the advantages of low cost, convenient adjustability, and precise operation. It is not suitable as a flight mount because it is not self-compensating for variation in mirror attitude or the direction of gravity forces.

Figure 2

MINISCUS MIRROR MOUNTING SCHEME

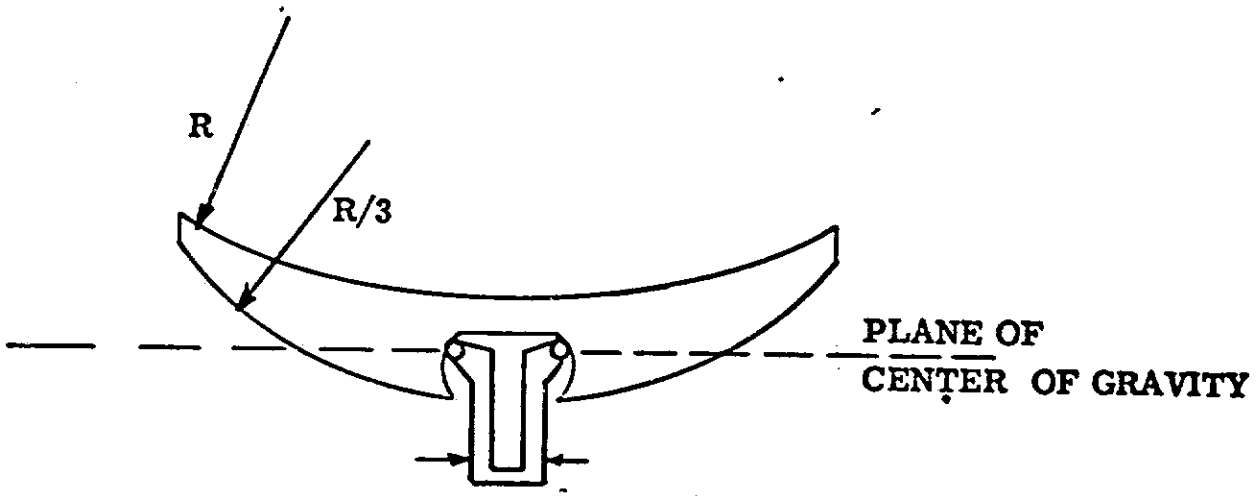

In general, the disadvantages of a solid mushroom design are by comparison:

1. The hub on the back is a potential fracture area, since all torques are constrained through the neck.
2. The hub adds weight.
3. The hub adds thermal mass.
4. Support is not at the center of gravity, which makes variable attitude testing and gravity release simulation more difficult to achieve.

It is suggested that the hub area of the mushroom mirror be redesigned to a configuration similar to that of the miniscus mirrors. This second mounting method is then viable from both an operational, testing and manufacturing point of view.

2.5 METROLOGY MOUNT CONCLUSIONS

The mount recommended by this report is the Stratoscope counterweighted mount. This has the advantages of past experience and proven performance. Moreover, it is very amenable to finite-element studies and can be computer modeled for residual deflections. The square array multi-point supports suggested in the preliminary study would give similar results but only for the horizontal position. The counterweighted mount works in any position. This is important for test simulating the balloon-borne portion of the heliograph mission.

All of the above indicates that the crucial element in the program will be the mount for the primary. Given a good mount, any of the designs will work and be of equal difficulty. However, the additional analytical studies required for the mushroom mirror and the risk of handling the requisite large number of support points on a design of nonuniform cross section, bring us to the conclusion that the solid and lightweight mirrors are preferable to a mushroom mirror from a metrology mount point of view.

3.0 MANUFACTURING RISK FACTORS

3.1 MANUFACTURING RISK FACTORS - SCOPE OF STUDY

In this task, elements of manufacturing risk associated with the primary mirror configuration selection were examined. These elements include grinding and polishing load deformations, amount of machining required, stress relief requirements, and requirements for new technology as applied to the manufacturing of the mirror configurations. In addition, the impact of bulk material parameters and tolerances on thermal and mechanical properties and on mirror performance were investigated.

3.2 GRINDING AND POLISHING LOAD DEFORMATIONS

Grinding and polishing load deformation of the mirror in a free state will vary as does the self-weight deflection. A mount which supports the mirror evenly enough to counter this self-weight deflection would prevent polishing and grinding load deformation. This is certainly true of solid mirrors, as experience has proven. It is also true of lightweighted mirrors, provided the size of the tool working the mirror is within smaller but acceptable limits.

Experience at Perkin-Elmer involves loads of about 35 to 40 pounds or 0.1 pound per square inch in manufacturing 27" lightweight mirrors. Applying the deflections formula used in paragraph 2.3, the load-deflection is linear. Thus, for a 260 pound mirror: $\frac{40}{260}$ = 15% of the residual deflection unaccounted for by the mount could be induced by tool loading. The mushroom mirror, again, due to the uncertainty of its mount has the most potential for load deformation. However, even in this case, 15% of the residual deflection should be inconsequential. (A sufficiently large number of support points is assumed.) Thus, polishing and grinding load deformation should not be a problem with any of the mirrors.

3.3 MACHINING REQUIREMENTS

The machining requirements and the resultant risk for the three mirror designs are directly proportional to the amount of material that must be

removed from the same original blank to achieve each final configuration. Starting with the same blank size then, the solid mirror would require the least machining, the cored lightweight the most, and the mushroom intermediate.

3.4 STRESS RELIEF

Stress relief considerations occur twice during the manufacturing process of the primary mirror.

The first instance of stress relief occurs during boule production of CerVit mirrors. Boules of CerVit are created by a casting process which can produce residual stresses during cooling of the cast boule. Much of this residual stress can be removed by the proper annealing (heat cycling) of the boules after casting; however, some residual stress will result.

Since all three candidate primary mirror configurations will be machined from approximately the same size boule, mirror configuration will have no impact on the amount of stress relief required in boule production nor the state of residual stress remaining in the boule after annealing. Thus, no mirror configuration affords an advantage in this consideration. However, for a given final level of residual stress, the mushroom mirror would be most adversely affected due to its lowest relative flexural strength.

The second instance of stress relief occurs following the machining of the mirror boules to the final configuration. Stress relief through acid etching of the machined surfaces is required to relieve the areas which are work-hardened by the machining process.

The impact that the three different configurations have in this regard is the amount of machining each requires. The greater the amount of machined surface, the greater the area that requires stress relieving; and the greater the resulting cost.

As low risk procedures are available to properly stress relieve each of the mirror configurations with no resultant damage, cost is the only factor which distinguishes the three configurations. Based on the amount

of surface area requiring stress relieving (and its resultant cost), the solid mirror configuration is most attractive, the lightweight mirror least attractive, and the mushroom mirror slightly behind the solid mirror. This factor taken alone is not of sufficient importance to influence the final mirror selection.

3.5 LOW SCATTER SURFACE REQUIREMENTS

New technology will be needed if a low scatter surface is required. A Mil-Spec scratch-dig specification of 120-70 is attainable as a normal shop practice while 60-40 is possible. A graph of surface code as a function of cost appears in Figure 3.

It should be noted, that scratch-dig code does not ensure a low scatter surface. "Orange peel" or other high frequency surface roughness created by the polishing process or by the surface characteristics of the substrate will create scatter many orders of magnitude greater than smooth 120-70 surfaces. The mirrors must be worked, using pitch laps with bowl fed slurry. Also, since the mirrors are to be polished to an aspheric surface, "relieved" or pliable laps need to be used to cope with the rapid curvature changes found in the surface of an aspheric. It is in this area that new technology is needed. It has been found at Perkin-Elmer in the manufacture of reticle quality grating blanks, that an 80-50 surface manufactured with a pitch lap on bowl feed will produce a very low scatter super smooth surface. However, similar blanks with 20-10 surfaces cloth polished produced unacceptably large amounts of scatter. The extension of pliable pitch lap methods to fast aspherics would greatly enhance the performance of this mirror.

None of the three mirror designs presents a singular need for this method of polishing. It would enhance all of them equally. Normal polishing methods were assumed for the study although it is anticipated that stray light suppression will be a major Photoheliograph requirement. Such a requirement does not impact this study.

Figure 3

CHANGE IN LABOR HOURS VS SURFACE CODE

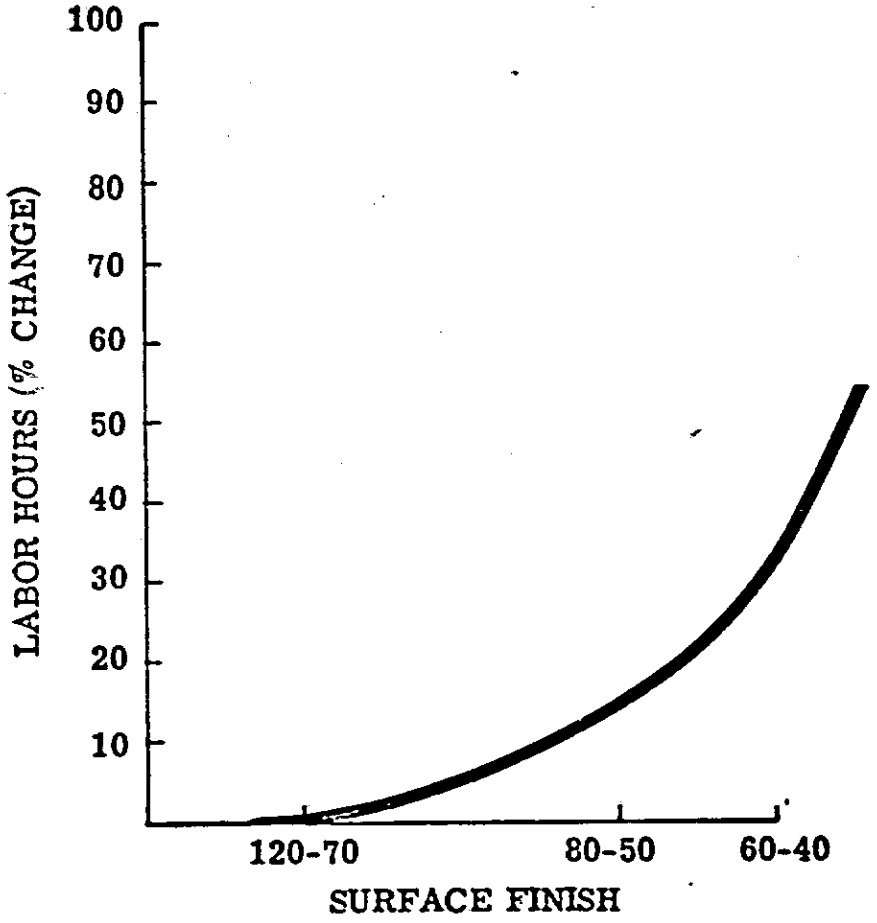

PERKIN-ELMER

3.6 MATERIAL PROPERTY VALUES AND THEIR TOLERANCES - EFFECT ON PERFORMANCE

In comparing the three primary mirror configurations made of CerVit, the material property absolute value and/or tolerance which most significantly affects relative mirror performance is the coefficient of thermal expansion (CTE) and its homogeneity.

The coefficient of thermal expansion of CerVit exhibits considerable variation. A typical boule will have CTE values in the range of 0 ± 0.03 ppm/°C. In addition the CTE variation in any boule cannot be predicted prior to casting. It can only be measured after casting.

The effect of this CTE value and its variation is to induce thermal distortions in the mirror under bulk average temperature changes and/or thermal gradients which may be greater than can be tolerated for specified performance.

In the absence of the ability to predict the CTE variation before casting, the best candidate among the three mirror configurations would be that whose performance is least affected by the CTE and its variations.

Assuming a particular identical CTE distribution for all three mirror configurations, i.e., a front to back CTE variation typical of CerVit, the thermal distortion for a unit bulk average temperature change is inversely proportional to the mirror thickness. Thus, the solid or cored mirrors are preferable to the mushroom mirror since their thickness is considerably greater than the effective thickness of the mushroom mirror.

A second consideration results from the fact that CerVit boules tend to have the greatest CTE variations just beneath their front and rear faces. The mushroom mirror's geometry requires the placement of its front face in this high CTE gradient region. Thus, even greater thermal distortions would be expected as compared with the solid and cored mirrors. With these, the high CTE gradient effect is averaged by the integrating effect of their greater thickness, i.e., the presence of other regions with lower CTE gradients.

Assuming identical CTE distributions, the solid and cored mirrors will exhibit identical distortion responses to bulk average temperature changes; thus, some other basis must be employed to compare their performance with regard to the CTE and its variation.

Thermal gradients directly influence thermal distortions and thus, mirror performance. Regions of large CTE variation induce distortions which can amplify the effects of the thermal gradients. Thus, both the thermal gradients and the CTE variations must be considered in comparing the two mirror designs.

A number of variables influence the relative thermal gradients that would be developed in each mirror, including: whether the mirror is being heated or cooled by the thermal control system, the types of mirror surface coatings, the types of environment, and the steady-state bulk average temperatures of each mirror. Different combinations of these variables can result in different relative thermal gradients; directly affecting choices between the two mirrors. Thus, variables must be specifically defined and evaluated before a choice can be made. Unfortunately, much of the information required to make this choice is not clearly defined at this point. However, a choice may still be possible based on some assumptions and approximate thermal analyses. These analyses indicate that the two mirrors must be cooled during operation. Assuming that the bulk average operational temperature of both mirrors is maintained at 72°F by rear face plate cooling; that both mirrors receive the same incident heat on the front faces; that both have the same front face coatings; that the pockets of the cored mirror have a highly reflective coating; then thermal analysis indicates that both mirrors will have the same order of magnitude of thermal gradient; and thus the resulting distortions will be of the same order.

This result would indicate that neither is a better choice. However, even if additional in-depth thermal/structural analyses are performed which indicate that the thermal distortions of both of the mirrors is acceptable, it may be a better choice to select the cored mirror over the solid. This is based on the fact that the CTE distribution of a cored mirror can be better determined than that for a solid mirror. Material samples can be taken from

the core of the cored mirror as well as from the circumference. This permits a more accurate prediction of mirror performance, directly reducing the risk involved with meeting the thermal distortion tolerance.

Therefore, although both solid and cored mirrors appear favorable, the final choice between the cored and solid mirror should be deferred until in-depth thermal structural analyses can be performed and other factors considered.

4.0 ULTIMATE QUALITY ASSESSMENT

4.1 ULTIMATE QUALITY ASSESSMENT - SCOPE OF STUDY

This effort consisted of two basic parts: (a) the determination of the relative cost versus surface figure for the three alternate mirror configurations, and (b) an assessment of the three mirror configurations.

The on-station performance assessment considered the following: thermal and temporal stability, weight, shock sensitivity, fundamental vibration modes and their interactions with expected control moment gyro operational frequencies.

4.2 COST VERSUS SURFACE FIGURE

The relative cost versus surface figure relationship was determined - see Figure 4. Assuming a good metrology support mount, the cost should not vary for the different mirrors, i.e., it is independent of mirror configuration.

4.3 ON-STATION PERFORMANCE

4.3.1 Thermal Stability

The purpose of this discussion is to comment on the thermal considerations which are relevant in comparing the primary mirror configurations of interest. The subject mirror is of CerVit, and is 100 cm in diameter. It is continuously irradiated by the sun, and is assumed to be cooled by means of a conditioning plate behind its rear surface. The configurations of interest are:

a. A solid mirror, approximately 6" thick.

b. A lightweight mirror with approximately a 6" total thickness.

c. A "mushroom" mirror, centrally mounted, with thickness varying from approximately 8" at the center hub to 1" at the edge.

The key areas to be considered in comparing the three configurations are as follows:

Figure 4

RELATIVE COST VS. SURFACE FIGURE

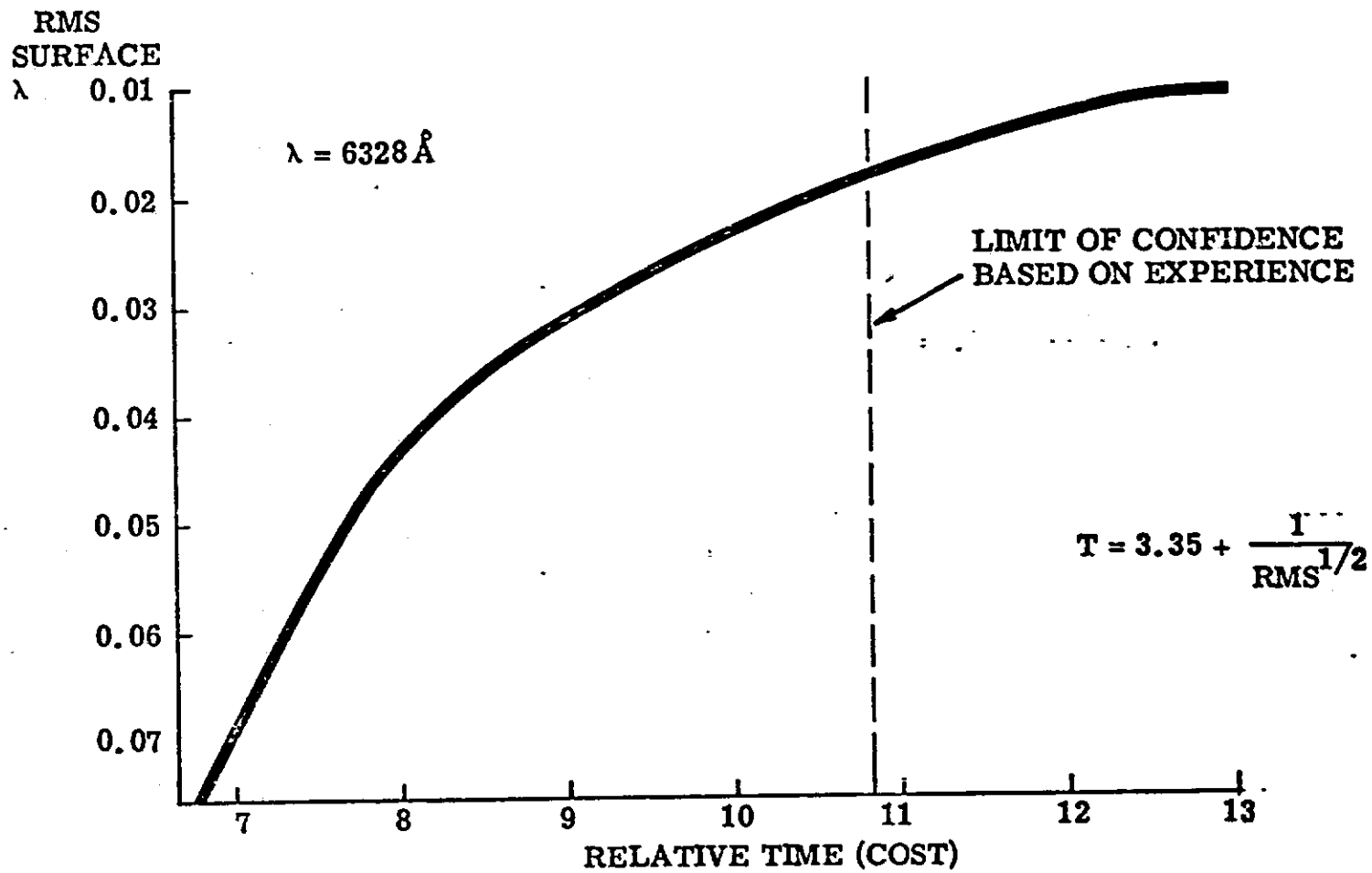

PERKIN-ELMER

a) Minimization of nonlinear thermal gradients resulting from the given heat load.

b) Minimization of the effects of nonuniform coefficient of thermal expansion (CTE).

c) Minimization of the effects of temporal variation in heat load.

Each of these key areas are discussed below.

Nonlinear Thermal Gradients

Nonlinear thermal gradients result in surface deformations whose effect on imagery is uncorrectable by refocussing. They are caused by a nonuniform heat flux to the mirror and/or by a nonlinear thermal resistance within the mirror. Since the former is equally applicable to the three mirror configurations, the basis for comparison should be the latter factor. From the viewpoint of uniformity of thermal resistance through and across the mirror, it is clear that the solid mirror is most favorable while the mushroom is least favorable. The lightweight mirror, with a diffuse core would tend to have higher gradients than the solid mirror. With a specular core, however, the gradients could be lowered substantially. In Figure 5, front to back temperature differences are shown for both a solid and a lightweight mirror with a specular core. For the simplified analysis which was conducted, the gradient through the lightweight mirror is less than that for the solid. This is because the effect of the specular core is to shunt the axial heat flow from the back of the faceplate directly to the control plate. Nonuniform heating which would cause radial and/or transverse gradients, however, would not be so effected, and for that case, the solid mirror would be superior. The axial gradients shown in Figure 1 are for a constant incident heat rate of 440 BTU/hr-ft^2 (one solar constant). For the solid and cored lightweight mirrors, the subject gradients are nominally linear. For the mushroom mirror, however, the axial gradient would be nonlinear, varying by a factor of about three from the edge to the region adjacent to the central hub.

Figure 5

MEAN TEMPERATURE AND FRONT TO BACK ΔT FOR SOLID AND LIGHTWEIGHT MIRRORS VS. CONTROL PLANE TEMP.

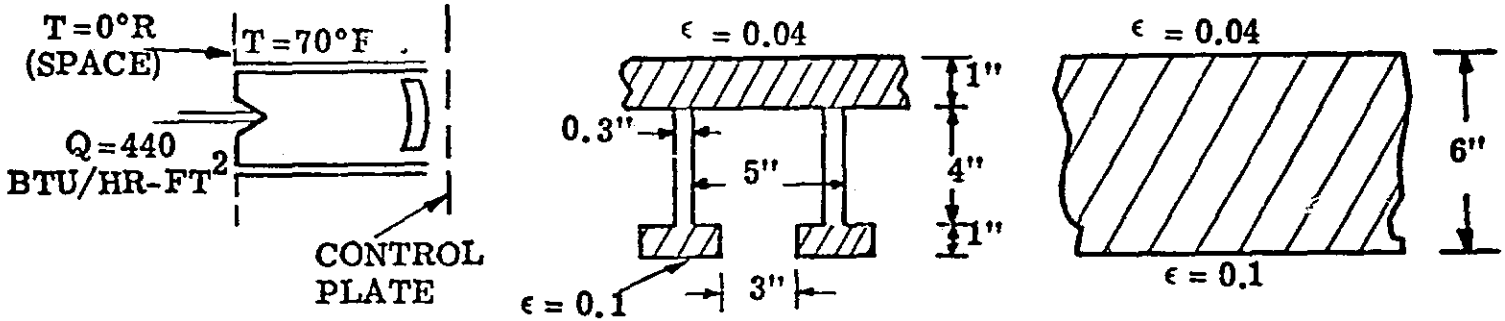

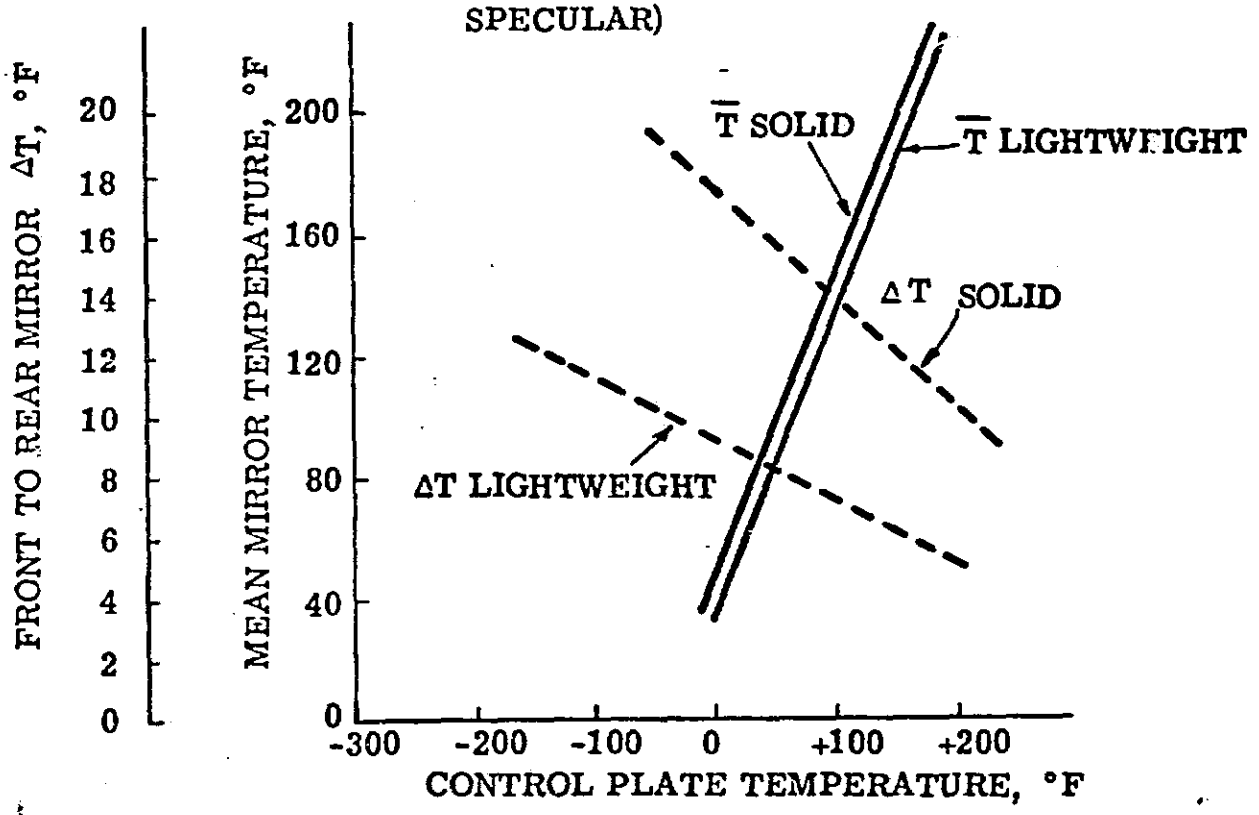

PERKIN-ELMER

Nonuniform CTE

The effect of a nonuniform CTE is analogous to the effect of a nonuniform temperature since surface deformation is, in general, a function of the product, $\alpha\Delta T$. Since a random variation in CTE will result in a surface figure error proportional to the mirror thickness, it is clear that for this case the mushroom mirror, being the thinnest, is preferable. Non-random variations are discussed in paragraph 3.6. If a random CTE variation having an rms value of $\pm 0.03 \times 10^{-6}$/°C is assumed, the allowable uniform temperature change corresponding to an rms surface error of 0.025λ is about ± 12° for a 6" thick mirror (solid or lightweight). For the mushroom mirror the allowable temperature change, if assumed to be proportional to thickness, would vary from about ± 9°F at the hub to about ± 72°F at the thin edge.

From Figure 5 it is seen that in order to keep the mirror temperatures within ± 12°F of an assumed fabrication temperature of 70°F, the control plate temperature would have to be maintained within approximate limits of 25 ± 12°F for the solid mirror and within approximately 40 ± 12°F in the lightweight mirror.

Temporal Variation on Heat Load

For orbital operation in which the heat load to the mirror is a time varying function, true steady-state conditions will never be realized, and both the mean mirror temperature, and the thermal gradients within the mirror will vary in a periodic fashion. Clearly it is beneficial to limit the amplitude of the variations. This can be done by the active thermal control system and/or by increasing the thermal time constant of the mirror. From the point of view of a large time constant, the solid mirror is obviously preferable, followed in order by the lightweight and the mushroom mirrors.

The normalized values of the thermal capacitances of the three mirror configurations are:

Solid	1.0
Lightweight	0.44
Mushroom	0.34

For a given periodic heat input, therefore, the amplitude of the temperature variations in the lightweight and mushroom mirrors will be about 2.3 and 2.9 times greater, respectively, than for the solid mirror.

Summary

The above discussion has attempted to present what are felt to be the principal thermal areas of consideration with regard to a comparison of the mirror configurations of interest. These are the areas which must be analyzed in depth before a choice can be made. Obviously such an in-depth analysis has not been made herein, and any conclusions at this time must be regarded as tentative. Nevertheless, it is felt at this time, that the single area of greatest risk with respect to a CerVit mirror is the potential image degradation resulting from random variations in the CTE. From this viewpoint, the mushroom configuration appears to be most favorable.

4.3.2 Temporal Stability

It has been found that the temporal stability of a mirror depends directly upon the proper removal of damaged areas resulting from the machining of the glass surfaces, i.e., the stress relieving via etching of these machined surfaces.

Thus, if any of the three mirror configurations was machined from a given boule; and then subjected to proper process control (stress relieving) its expected temporal stability should not be different than any of the other candidate configurations.

Proper process control procedures exist for all three mirror configurations. The only difference between the three is the amount of stress relieving required (a direct function of the amount of machining required), and the resultant impact on cost to produce the same temporal stability. Thus, from a cost point of view and its affect on temporal stability, the solid mirror is most advantageous, with the mushroom mirror next, and the cored mirror least desirable.

It should be noted, however, that this cost factor, taken alone, is not of sufficient importance to allow a choice to be made between the three mirror candidates.

4.3.3 Weight

It is felt that the weights given for the three mirror configurations (solid, 611 lbs.; cored, 272 lbs.; mushroom, 208 lbs.) are reasonable values and compare favorably with similar state-of-the-art designs produced by Perkin-Elmer.

If total system weight is a critical design parameter, the clear choice is the lightest mirror - the mushroom configuration; with the solid mirror being the least desirable.

It should be mentioned that although the given weight for the cored, lightweight mirror is similar to the mushroom mirror and thus might appear quite attractive; its true, finished weight will be slightly higher due to the requirement for stress level reduction to meet shock loads, see paragraph 4.3.4. This additional weight will result from thicker ribs and faceplates in the mirror mounting areas. It is felt, however, that this additional weight should not greatly deter from its attractiveness when compared with the other two configurations. Thus, from a minimum weight point of view, the cored, lightweight mirror may be a viable alternative for the mushroom mirror; and clearly more attractive than the solid mirror.

If weight is of minimal importance, other factors such as production cost should dominate in the selection between the three mirrors.

4.3.4 Shock Sensitivity

The three mirror configurations were analyzed to determine the maximum resulting stress levels under worst case loading conditions, i.e., their shock sensitivities.

The worst case loading condition occurring during either the Balloon flight or the Shuttle flight for structures qualified by test is the Shuttle crash landing loading condition which induces an ultimate load of 9-G normal to the face of the mirror (Ref: "Shuttle Payloads Accommodations Document", NASA, Johnson Space Flight Center). This loading condition carries with it a required factor of safety of 1.0 and a required margin of safety of 0.0, i.e., the structure must simply hold together; but buckling and yielding are permissible.

The ultimate strength of CerVit glass employed for this analysis was 500 psi. Perkin-Elmer has traditionally employed a 1000 psi maximum ultimate strength - a value known by experience to be sufficiently low to avoid fracture-mechanics type failures that are associated with brittle materials like CerVit. However, a recent report by Keto Soosaar of MIT Draper Lab for NASA, Marshall Space Flight Center ("LST 3 Meter Mirror Final Report", dated December 1974), suggests that until further material strength and fracture-mechanics investigations are done on CerVit and ULE glasses, the ultimate strength of these materials should be limited to 500 psi. It should be noted that this corroborates the earlier recommendations of Corning Glass for ULE type large optical elements. In deference to the above reports, the allowable ultimate strength was lowered as mentioned above.

The mounting scheme chosen for each mirror configuration was that which in Perkin-Elmer's experience appears most viable for the Shuttle Mission. In particular, the solid and cored mirrors would have a three point rim support with axial and tangential restraint; while the mushroom mirror would have a central hub mount. It is known that these mounting schemes are not optimum from a self-weight deflection point of view; but since 1-G operation is not part of the Shuttle Mission, these simpler, less costly, mounting arrangements are more desirable.

Table 2 contains the self-weight deflection of the three mirror configurations mounted as described above. These results point out the obvious expectation that 1-G operation (as in the Balloon flight) requires a multi-point support similar to a metrology mount (discussed elsewhere in this report) - which drastically reduces both 1-G deflection and induced stresses.

Table 4 contains the resulting stress levels for the three mirror configurations in their Shuttle Mission, mounting configuration subject to the 9-G Shuttle crash landing loading. These results point out that the solid and mushroom mirrors have acceptable stress levels, while the cored, lightweight mirror is overstressed.

This overstressed condition exists only in the mount areas and can be easily remedied by thickening the mirror faceplates and the core ribs in these

Table 4

PRIMARY MIRROR SHOCK SENSITIVITY

9G-SHUTTLE CRASH LANDING LOADING SHUTTLE MISSION MOUNTING SCHEME

- o SOLID – 3 POINT SUPPORT
- o CORED, LIGHTWEIGHT – 3 POINT SUPPORT
- o MUSHROOM – CENTRAL, HUB MOUNT

FACTOR OF SAFETY = 0.0
MATERIAL = CERVIT
ULTIMATE STRENGTH = 500 PSI

MIRROR CONFIGURATION	MAXIMUM STRESS (PSI)	MARGIN OF SAFETY
SOLID	157	+2.18
CORED, LIGHTWEIGHT	776*	-0.36**
MUSHROOM	449	+0.11

*374 PSI for ULE Design.

**M. S. = +0.29 for ULE Design.

localized areas. In particular, doubling the faceplate thickness and the web thickness will lower the resulting stresses to acceptable levels with only a small weight penalty.

A second alternative is to employ ULE eggcrate construction instead of the CerVit cored construction. This change eliminates the rear faceplate holes and their associated stress concentration, and results in the reduction of the mirror bending stress by a factor of 3. This stress reduction removes the requirement for any faceplate or web stiffening at the mounts - thereby avoiding the additional weight and surface stiffness discontinuities associated with a mount-stiffened, cored, CerVit design.

If the above changes are incorporated in the cored, lightweight mirror design, then all three mirror configurations would be acceptable from a shock sensitivity point of view; otherwise only the mushroom and the solid configurations are acceptable.

4.3.5 Minimum Natural Frequency

The minimum natural frequency of each of the primary mirror configurations was determined to detect any possible interactions with the expected CMG vibrational frequencies. Typical CMG vibrational frequencies are in the range of 100-150 Hz. Good mirror design has the minimum natural frequency of a mirror considerably higher than the expected CMG vibrational frequency to avoid any possible interaction.

The minimum natural frequencies for each of the mirror configurations will result from the Shuttle Mission mounting configurations (solid and cored, lightweight - 3 point rim support; mushroom - central hub support) which provides the minimum number of support points-allowing the greatest self-weight deflection (lowest spring constant); and thus, minimum natural frequencies. If these minimum natural frequencies experience no interaction with the CMG vibrational frequencies; then it follows that any Balloon Mission mount, which must be stiffer (higher natural frequency) to allow 1-G operation; will also experience no CMG vibrational frequency interaction.

Table 5 contains the results of this analysis. The results indicate that the minimum natural frequency of all configurations are much higher than the CMG vibrational frequencies; implying no interaction and allowing the conclusion that all three configurations are acceptable from a vibration point of view.

Table 5

PRIMARY MIRROR MINIMUM NATURAL FREQUENCY

SHUTTLE MISSION MOUNTING CONFIGURATIONS

- o SOLID – 3 POINT SUPPORT
- o CORED, LIGHTWEIGHT – 3 POINT SUPPORT
- o MUSHROOM – CENTRAL, HUB SUPPORT

EXPECTED CMG VIBRATIONAL FREQUENCIES: 100 - 150 Hz

MIRROR CONFIGURATION	MINIMUM NATURAL FREQUENCY (Hz)
SOLID	678
CORED, LIGHTWEIGHT	452
MUSHROOM	264

- o ABOVE RESULTS INDICATE NO CMG VIBRATIONAL FREQUENCY FOR ALL THREE MIRROR CONFIGURATIONS

5.0 GENERAL CONCLUSIONS AND RECOMMENDATIONS

The preceding paragraphs have compared the three primary mirror configurations for a number of different parameters. Relative performances of the three mirrors varied for the different parameters with no single configuration exhibiting either an outstanding or a severely degraded performance, as compared with the others.

A single final recommendation is required as the final output of the study. To accomplish this, a rating scheme was devised as outlined below. It considers the relative performances of the mirrors for each parameter and allows a quantitative method of making the final recommendation.

It should be noted that the evaluation matrix assumes weighting factors for the particular application to make the general comparison of the characteristics of the three mirror types. Each of the mirror types has specific advantages and disadvantages. For another specific application, the weighting factors might assume such values that another of the three mirror types could be selected as superior. That is, selection of the best mirror type for a specific application requires evaluation of weighting factors for that specific application.

5.1 PARAMETER VERSUS MIRROR CONFIGURATION MATRIX

To arrive at a final recommendation of mirror configuration, a matrix was established - see Table 6 - of the factors considered in the mirror study. Each factor was assigned a maximum point value based on its relative importance in the mirror selection process; with the total number of points taken as 100.

Each mirror configuration will be assigned a number of points for each parameter considered based on its relative performance in this area as compared with the others, and the resulting difficulty in achieving minimum required performance. The mirror scoring the highest total number of points will be the final recommended design.

This elimination process does not allow for design deficiencies which alone would call for immediate rejection of the design, i.e., an overstressed

TABLE 6

PARAMETER VS. MIRROR CONFIGURATION MATRIX

Task	Parameter	Weighting Factor Maximum Value	Candidate Mirror Configuration		
			Solid	Standard Lightweight	Mushroom
Manufacturing Metrology (Mount)	Cost	8			
	Risk Factors	8			
	Manufacturing Schedule Req't's.	3			
	Simulation Of G-Release	8			
	Sub-Total	27			
Manufacturing Risk Factors	Grinding/Polishing Load Deformation	8			
	Machining Requirements	8			
	Stress Relief	4			
	Requirements For New Technology	5			
	Material Property Effects On Performance	8			
	Sub-Total	33			
Ultimate Quality Assessment	Cost Vs. Surface Figure	8			
	On-Station Performance Effects: Thermal Stability	8			
	On-Station Performance Effects: Temporal Stability	3			
	On-Station Performance Effects: Weight	5			
	On-Station Performance Effects: Shock Sensitivity	8			
	On-Station Performance Effects: Vibration Modes CMG Interaction	8			
	Sub-Total	40			
	Totals	100			

mirror. In such instances, if design changes can be suggested which remove the design deficiency, the incorporation of these changes into the design will be assumed and this final design used in the rating process. However, if no changes can be offered to remove the design deficiency, then the design will be rejected and the elimination process used for rating the remaining mirror configurations as outlined above.

5.1.1 Guidelines for Point Assignment

A set of guidelines were established to aid in completing the "Parameter vs. Mirror Configuration" Matrix, as follows:

1) The configuration achieving the best performance with the least difficulty achieved the maximum number of points assigned to that parameter, with the others downgraded proportionally.

2) Achievement of minimum performance was assumed for all parameters other than the one under consideration to avoid doubly penalizing a mirror for lack of performance in one area which affects the performance of the mirror for the parameter under consideration. An example of this occurred in the area of the metrology mount where the mushroom mirror was downgraded for difficulty in achieving minimum desired intersupport deflection; but, achievement of this minimum was assumed when considering the grinding/polishing load deformations which assumes a metrology mount having minimum performance.

3) If all three mirror configurations achieved the minimum required performance for the parameter, then the three mirrors were judged based upon their relative performance above the minimum required value.

4) If one of the mirror configurations met the required performance, the difficulty and risk achieving this minimum acted as the basis for assigning points.

5.2 CONCLUSIONS

Based upon the above guidelines, the "Parameter vs. Mirror Configuration" Matrix discussed in paragraph 5.1 was completed - see Table 7. The results indicate relatively close total point values for the three mirrors - i.e., 92, 81 and 70 points for the solid, lightweight and the mushroom mirror; respectively.

The closeness in total point value resulted from the fact that the three mirrors received similar overall ratings for "Manufacturing Risk Factors" and for "Ultimate Quality Assessment" with the greatest difference in the "Metrology Mount" section where a factor of two differences occurred in the total points between the mushroom mirror and the other two configurations reflecting the difficulty in achieving the same metrology mount deflection performance from a thin tapered mirror as can be achieved with the solid and lightweight mirror configurations.

Basically, these results point out that the three mirror configurations have essentially equal qualities as far as "On-Station" performance and "Manufacturing Risk" are concerned, with slight advantages and disadvantages essentially canceling each other.

The major difference between the three configurations occurs as a result of the geometry of the mushroom mirror. Its thin tapered shape possesses lower flexural rigidity and a nonuniform weight distribution. This necessitates much greater in-depth analytical and design studies to design a metrology mount whose intersupport deflections meet the required levels with a high degree of confidence. This shape also requires new tooling equipment and the training of manufacturing personnel which would not be required for the more conventional solid and lightweight designs.

The main differences between the solid and lightweight mirrors result from the presence of the cored out areas of the lightweight mirror. The coring process adds to the amount of machining and stress relief required and adds flexibility, making metrology mount designs more complicated. It lowers shock

TABLE 7

PARAMETER VS. MIRROR CONFIGURATION MATRIX

Task	Parameter	Weighting Factor Maximum Value	Candidate Mirror Configuration		
			Solid	Standard Lightweight	Mushroom
Manufacturing Metrology (Mount)	Cost	8	8	7	3
	Risk Factors	8	8	7	3
	Manufacturing Schedule Reqt's.	3	3	3	3
	Simulation Of G-Release	8	8	8	3
	Sub-Total	27	27	25	12
Manufacturing Risk Factors	Grinding/Polishing Load Deformation	8	8	8	8
	Machining Requirements	8	8	5	6
	Stress Relief	4	4	3	2
	Requirements For New Technology	5	5	5	5
	Material Property Effects On Performance	8	7	8	6
	Sub-Total	33	32	29	27
Ultimate Quality Assessment	Cost Vs. Surface Figure	8	8	8	8
	On-Station Performance Effects: Thermal Stability	8	4	4	8
	On-Station Performance Effects: Temporal Stability	3	3	1	2
	On-Station Performance Effects: Weight	5	2	4	5
	On-Station Performance Effects: Shock Sensitivity	8	8	4	4
	On-Station Performance Effects: Vibration Modes CMG Interaction	8	8	6	4
	Sub-Total	40	33	27	31
	Totals	100	92	81	70

resistence, temporal stability and natural frequencies. These are all to the detriment of the lightweight mirror as seen in the total ratings.

In conclusion, the closeness in the total points scores of each mirror indicates that each has a sufficient number of good qualities that when integrated with its negative properties produce three mirrors of almost equal attractiveness. However, the additional design costs and risks associated with the metrology mount for the mushroom mirror (not required by the others) reduces its attractiveness and forces the final recommendation that the solid mirror is the best choice, followed by the lightweighted configuration and, lastly, by the mushroom mirror.

APPENDIX A

SELF-WEIGHT DEFLECTION OF 65 AND 100 CM MUSHROOM MIRRORS

ATTACHMENT

1. Self-Weight Deflection Analysis, 65 cm (26.12") Diameter JPL Mushroom Mirror
2. Self-Weight Deflection of a 100 cm (40") Diameter Mushroom Mirror Through Scaling Laws
3. Self-Weight Deflection Analysis via Tapered-Beam Method - 100 cm (40") Diameter Mushroom Mirror

REFERENCE

a. Report 750--7; Rev. A, "Photoheliograph Primary Mirror Development", dated April 7, 1969, Jet Propulsion Laboratory

SUMMARY

As a result of a request by NASA, Goddard; the self-weight deflection predictions made by both JPL and Perkin-Elmer for 65 and 100 cm diameter mushroom mirrors were compared and found to provide similar results.

INTRODUCTION

The self-weight deflection of a 100 cm mushroom mirror was determined as part of the Solar Photoheliograph Study for NASA, Goddard. Through use of an approximate closed-form solution, the self-weight deflection was determined as of the order of 8.8λ (λ 6328Å) - see Attachment 3.

DISCUSSION

These results were presented to NASA, Goddard as part of the preliminary output of the above study. Their response indicated that the Jet Propulsion Laboratory had evaluated this mirror in the past and their results indicated

that the self-weight deflection was of the order of milliwaves and not waves. They also indicated that the milliwave result was doubtful but would like Perkin-Elmer to explain the difference.

To settle this discrepancy, a copy of the JPL report which presented this information - Reference A - was obtained and reviewed. Three conclusions were drawn from this review:

a. JPL's figure was for a 65 cm and not a 100 cm mirror.

b. The results of this evaluation are not directly comparable.

c. Perkin-Elmer's approximate analysis techniques predict results of the same order of magnitude as JPL's computer solution.

These conclusions will be further discussed below.

JPL performed a finite-element computer solution for the self-weight deflection of a 65 cm mushroom mirror. Their results were presented in two forms: absolute deflection values and "O.P.D." values of the order of milliwaves. It is this latter result which NASA compared with the "absolute" deflection numbers presented by Perkin-Elmer in the 100 cm Solar Photoheliograph Mushroom Mirror Study.

Although the above generally explains away most of the discrepancy that existed, it was felt that an additional effort should be made to establish confidence in the Perkin-Elmer self-weight deflection techniques - especially as applied to the 100 cm mushroom mirror which JPL did not evaluate. This effort is further justified by the fact that the 100 cm mirror deflection values presented to NASA were based on an approximate closed-form solution owing to the lack of funds to perform a computer solution and to the unavailability of a suitable exact, closed-form solution.

To establish the required confidence in the approximate analysis techniques, two separate analyses were performed as follows: a) The Perkin-Elmer approximate techniques were applied to the same 65 cm mushroom mirror that JPL

evaluated with their computer solutions and the results compared - see Attachment 1 and b) the JPL computer results for the 65 cm mushroom mirror evaluated by Perkin-Elmer and the results compared - see Attachment 2. An adequate performance criterion for the Perkin-Elmer approximate techniques was taken as its ability to predict self-weight deflections of the same order of magnitude as the computer solutions. This proved to be the case in both of the above analyses with any remaining differences between the approximate and computer solutions attributed to the simplifying assumptions made in the approximate solutions. The conclusion could then be drawn that the Perkin-Elmer approximate techniques can be used with confidence for the purpose for which they were applied.

CONCLUSION

As a result of the above efforts, it can be finally concluded that Perkin-Elmer and JPL agree on the deflections of mushroom mirrors providing they are presented in the same form.

APPENDIX A

ATTACHMENT 1

SELF-WEIGHT DEFLECTION ANALYSIS
65 CM (26.12") DIAMETER JPL MUSHROOM MIRROR

BY ..... DATE ..... SUBJECT ..... SHEET NO. ..... OF .....
CHKD. BY ..... DATE ..... JOB NO. .....

SELF-WEIGHT DEFLECTION ANALYSIS

26.12" DIA. JPL - MUSHROOM MIRROR

HUB - MOUNTED

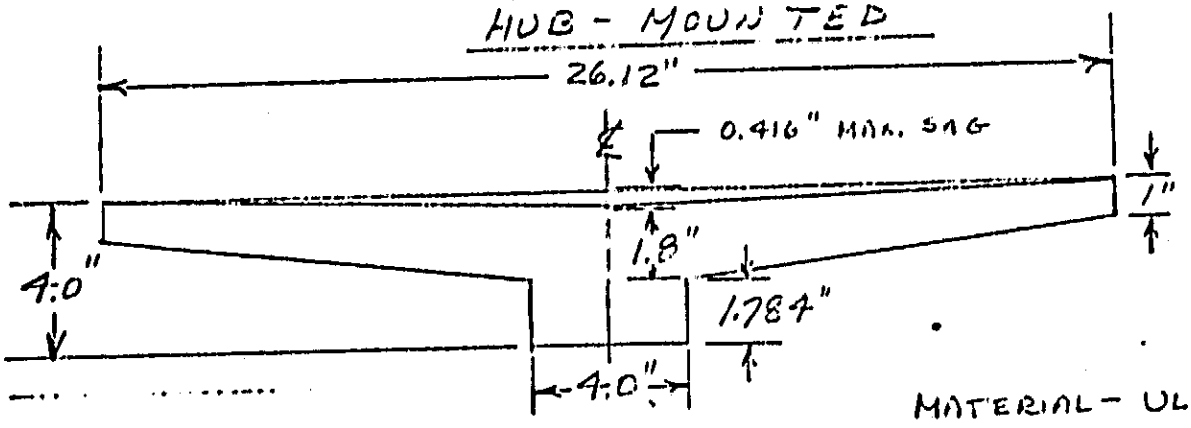

MATERIAL - ULE FUSED SILICA

REFERENCE FOR ABOVE DESIGN:

CONFIGURATION NO. 1 - FIGURE 2 - "PRIMARY MIRROR CONFIGURATION IDENTIFICATIONS

PAGE 7, AND PAGES 34 (COMPUTER MODEL)

JET PROPULSION LABORATORY REPORT # 750-7, REV A

"PHOTOHELIOGRAPH PRIMARY MIRROR DEVELOPMENT"

DATED APRIL 7, 1969

SELF-WEIGHT DEFLECTION OF ABOVE MIRROR AS DETERMINED BY JPL COMPUTER SOLUTION

REF - JPL REPORT (ABOVE):

PAGE 7, TABLE 7 - "SUMMARY OF THE COMPUTER ANALYSES ON THE PHOTOHELIOGRAPH MIRROR"

RUN # 2 - "1G LOAD - MIRROR SUPPORT DOWN"

MAXIMUM DEFLECTION (JPL) = 22.372×10^{-6} INCHES

BY.....DATE..... SUBJECT..... SHEET NO.....OF.....

CHKD. BY.....DATE..... JOB NO.....

Plane-End Self-Weight Deflection Of 26.12" Dia. Aluminum Mirror Hub Mounted

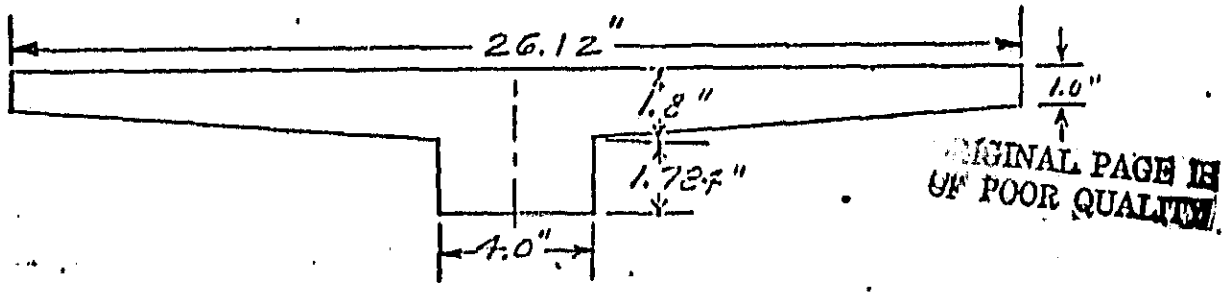

Note- Ignore Curvature Of Front Face Of Mirror

For Analysis Purposes, Consider A 1° Radial Segment Of The Mirror As A Doubly-Tapered Cantilever Beam With The Central Hub As Rigid.

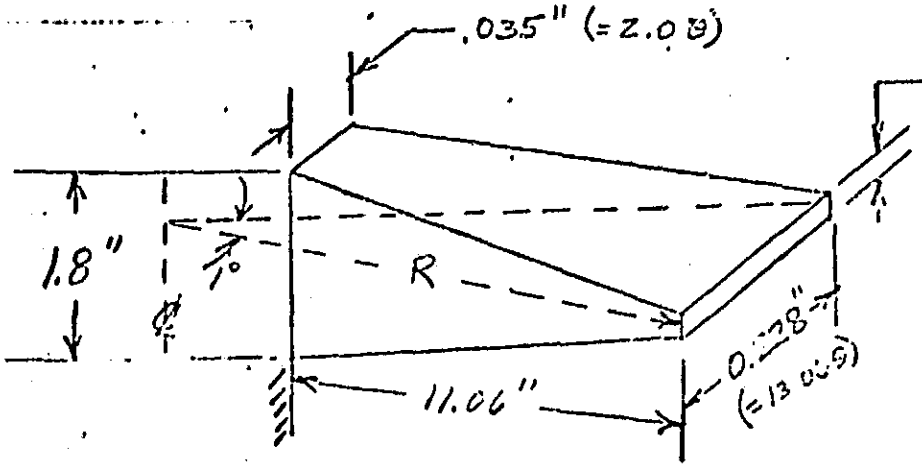

R= 13.06"

Not To Scale

Cantilever Beam Model

BY_____DATE_____ SUBJECT_____ SHEET NO.____OF____

CHKD. BY_____DATE_____ JOB NO._____

CONSIDER THE FOLLOWING BEAM MODEL

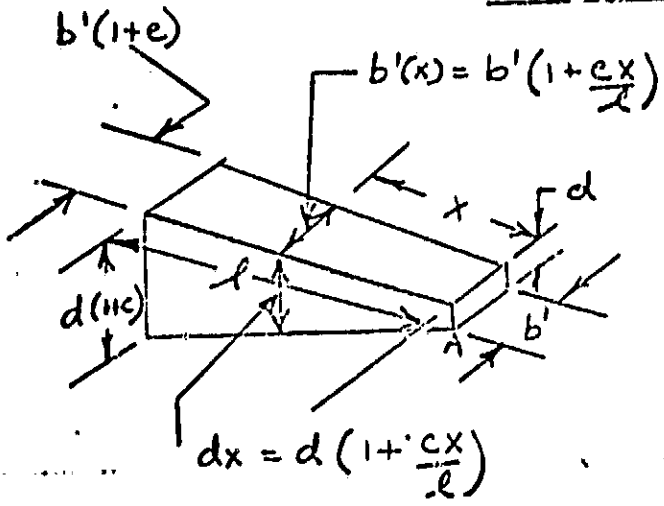

$$I_A = \frac{1}{12} b' d^3 = I$$

$$I_x = I\left(1+\frac{e}{\ell}x\right)\left(1+\frac{c}{\ell}x\right)^3$$

$$A(x) = b'd\left(1+\frac{ex}{\ell}\right)\left(1+\frac{cx}{\ell}\right)$$

FOR SELF-WEIGHT LOADING, $w = f(x) = -\rho A(x)$ #/in

CONSERVATIVELY, APPLY $w_{max} = \rho A_{max}$ TO BEAM MODEL AS A UNIFORM LOAD

TO DETERMINE A_{max}

$$\frac{dA(x)}{dx} = 0 = \left(\frac{e+c}{\ell}\right) + \frac{2ecx}{\ell^2}$$

$$\boxed{x = -\left(\frac{e+c}{\ell}\right)\left(\frac{\ell^2}{2ec}\right) = -\left(\frac{e+c}{2ec}\right)\ell}$$

BY _____ DATE _____ SUBJECT _____ SHEET NO. _____ OF _____

CHKD. BY _____ DATE _____ JOB NO. _____

To Determine e, c, l For This System

$b'(1+e) = 2.0"\ \theta$
$b' = 13.06"\ \theta$
$\Rightarrow 1+e = \frac{2.0}{13.06}$, $e = -.847$

$d(1+c) = 1.8"$
$d = 1.0"$
$1+c = 1.8$, $c = 0.8$

For: $l = 13.06 - 2.0 = 11.06$
$e = -0.847$
$c = 0.800$

$$x = -\left(\frac{e+c}{2ec}\right) l = -\left\{\frac{-0.847+0.800}{2(-0.847)(0.800)}\right\}\{11.06\} = -0.35"$$

Since the beam model terminates @ x=0, implying no beam stations for negative values of x, the above solution for maximum actual station is not useful. In light of this result, a "relative" maximum must be determined for the beam. This can be accomplished either through a trial and error process or by inspection. For purposes of clarification, a trial and error procedure will be employed in which a number of

BY.....DATE..... SUBJECT..... SHEET NO.....OF.....

CHKD. BY.....DATE..... JOB NO.....

STATION VALUES WILL BE SELECTED AND TABLE WILL BE CALCULATED, WITH THE RELATIVE MAXIMUM BEING TAKEN AS THE LARGEST AREA DETERMINED BY THIS PROCEDURE:

STATION, x	AREA $= A(x) = b'd\left(1+\frac{c_x}{c}\right)\left(1+\frac{c_y}{c}\right)$
0	$(13.06\,\Theta)(1.0) =$ $13.06\,\Theta$
$\ell/4$	$(13.06\,\Theta)\left(1-\frac{0.547}{4}\right)(1.0)\left(1+\frac{0.3}{4}\right) =$ $12.35\,\Theta$
$\ell/2$	$(13.06\,\Theta)\left(1-\frac{0.547}{2}\right)(1.0)\left(1+\frac{0.3}{2}\right) =$ $10.54\,\Theta$
$\frac{3\ell}{4}$	$(13.06\,\Theta)\left(1-\left[\frac{3}{4}\right][0.547]\right)(1.0)\left(1+\left[\frac{3}{4}\right][0.3]\right) =$ $7.62\,\Theta$
ℓ	$(13.06\,\Theta)(1-0.547)(1.0)(1+0.3) =$ $3.6\,\Theta$

AS EXPECTED, THE MAXIMUM AREA OCCURS @ $X=0$

$$\Rightarrow A_{MAX} = b'd = (13.06\,\Theta)(1.0) = (13.06)\left(\tfrac{1}{32^2}\right)(1.0) =$$

$$= 0.228 \text{ IN}^2$$

$$W_{MAX} = \rho A_{MAX} = (.08\ \#/\text{IN}^3)(0.225\ \text{IN}^2) = 0.018\ \#/\text{IN}$$

ULE

→ APPLY AS A UNIFORM LOAD TO TAPERED BEAM

BY.....DATE..... SUBJECT..... SHEET NO.....OF.....

CHK'D. BY.....DATE..... JOB NO.....

1-6- Self-Weight Deflection

Considering the 1° radial segment beam with a uniform loading of 0.018 #/in

$$\Delta_{\substack{MAX \\ SELF-WT}} = \left[\frac{wl^4}{2EI}\right]\left[\frac{(3c-2e)}{c^2(e-c)^2(1+c)} + \frac{(2+c)}{2c^2(e-c)(1+c)^2} - \frac{\ln(1+c)}{e(e-c)^3} + \right.$$

$$\left. + \frac{e^2-3c(e-c)}{c^3(e-c)^3}\ln(1+c)\right] = K\frac{wl^4}{EI}$$

where: $I = \frac{1}{12}b'd^3$ (see P. 3).

For: $w = 0.018$ #/in

$l = 11.06$" (cf P4)

$E = 9.8\times10^6$ psi (U.L.C.)

$I = \frac{1}{12}b'd^3 = \frac{1}{12}(0.228)(1.0)^3 = 0.019$ in^4

$c = 0.8$

$e = -0.847$ } (c.f. P. 4)

$$\Delta_{\substack{MAX \\ SELF-WT}} = \left[\frac{(0.018)(11.06)^4}{2(9.8\times10^6)(0.019)}\right]\left[\frac{3(0.8)-2(-0.847)}{(0.8)^2(-0.847-0.8)^2(1+0.8)} + \frac{(2+0.8)}{2(0.8)^2(-0.847-0.8)(1+0.8)^2}\right.$$

$$- \frac{\ln(1-0.847)}{(-0.847)(-0.847-0.8)^3} +$$

$$\left. + \frac{(-0.847)^2-3(0.8)(-0.847-0.8)}{(0.8)^3(-0.847-0.8)^3}\ln(1+0.8)\right]$$

$$\Delta_{\substack{MAX \\ SELF-WT}} = \left[1446.482 \times 10^{-6}\right]\left[\frac{4.094}{5.124} + \frac{2.8}{-6.630} - \frac{-1.577}{3.764} + \frac{(4.670)(.588)}{-2.257}\right]\left[\frac{1}{2}\right]$$

$$= \left[1446.482 \times 10^{-6}\right]\underbrace{\left[1.310 - 0.410 + 0.496 - 1.201\right]}_{K = .097}\left[\frac{1}{2}\right]$$

$$= 141 \times 10^{-6} \text{ in} =$$

@ 6328 Å, $\lambda = 25 \times 10^{-6}$

$$\underline{\Delta_{SELF-WT} = 5.6\lambda}$$

The above deflection is considerably greater than the 22×10^{-6} in predicted by JPL. The discrepancy can be attributed to two main factors: a) a one-dimensional solution was employed for a two dimensional problem - which ignores the existence of hoop (tangential) stiffness of the mirror, and b) a uniform loading distribution equal to the maximum local weight was employed.

The second of these two factors can be improved upon by revising the loading distribution to one that more accurately resembles the

True Loading distribution. Study Of The Area/Weight Distribution - See P. 5 - Allows The Conclusion That The Distribution Is More Like The Superposition Of A Uniform And A Triangular Distribution As Follows:

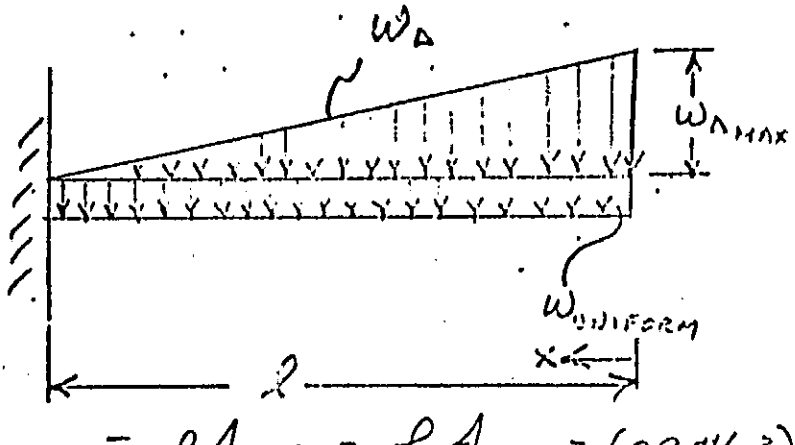

$$w_{UNIFORM} = \rho A_{MIN} = \rho A_{x=\ell} = (.08\ \#/in^3)(3.60)\left(\frac{1}{57.3}\right) = .005\ \#/in$$

$$w_{\Delta_{MAX}} = \frac{\rho(A_{MAX} - A_{MIN})}{\ell} = \frac{\rho(A_{x=0} - A_{x=\ell})}{\ell} =$$

$$= \frac{(.08\ \#/in^3)[13.06 - 3.6]\left[\frac{1}{57.3}\right]}{11.06''} = .001\ \#/in^2$$

$$\Delta_{SELF-WT} = \Delta_{\substack{UNIFORM \\ LOAD}} + \Delta_{\substack{TRIANGULAR \\ LOAD}}$$

Determine $\Delta_{\substack{UNIFORM \\ LOAD}}$

Ratio Original Solution (see P. 6-7)

$$\Delta_{UNIFORM} = \left(\frac{.005}{.018}\right)(141 \times 10^{-6}\ in) = 39.2 \times 10^{-6}\ in$$

BY _____ DATE _____ SUBJECT _____ SHEET NO. 1 OF 2

CHKD. BY _____ DATE _____ JOB NO. _____

DETERMINE $\Delta_{\text{TRIANGULAR LOAD}}$

$$\Delta_{\text{TRIANGULAR LOAD}} = \frac{w l^4}{EI}\left[K - K'\right]$$

where: $w = w_\Delta \, l$ (#/in)

K = UNIFORM LOAD FACTOR = .097 (SEE P 7)

$$K' = \frac{1}{6}\left[\frac{3e-4c}{c^3(e-c)^2(1+c)} - \frac{2+c}{2c^3(e-c)(1+c)^2} + \frac{\ln(1+c)}{e^2(e-c)^3} + \right.$$

$$\left. - \frac{6c^2-8ec+3e^2}{c^4(e-c)^3}\ln(1+c) + \frac{1}{ec^3}\right]$$

For $e = -0.847$, $c = 0.800$

$$K' = \frac{1}{6}\left[\frac{(3)(-0.347)-4(0.8)}{(0.8)^3(-0.847-0.8)^2(1+0.8)} - \frac{2+0.8}{2(0.8)^3(-0.847-.8)(1+0.8)^2} + \right.$$

$$+ \frac{\ln(1-0.847)}{(-0.847)^2(-.847-.8)^3} - \left\{\frac{6(.8)^2-8(-.847)(.8)+3(-.847)^2}{(0.8)^4(-.847-.8)^3}\right\}\ln(1+.8) +$$

$$\left. + \frac{1}{(-.847)(0.8)^3}\right] =$$

$$= \frac{1}{6}\left[\frac{-5.741}{2.5} - \frac{2.8}{-5.464} + \frac{-1.877}{-3.205} + \right.$$

$$\left. - \left\{\frac{3.84+5.421+2.152}{-1.830}\right\}(0.588) - 2.306\right]$$

$$= \frac{1}{6}\left[-2.296 + 0.512 + 0.586 + 3.667 - 2.306\right]$$

$$K' = \frac{1}{6}\left[0.163\right] = .027$$

BY _____ DATE _____ SUBJECT _____ SHEET NO. ____ OF ____

CHKD. BY _____ DATE _____ JOB NO. _____

$$\Delta_{\substack{\text{TRIANGULAR}\\\text{LOAD}}} = \frac{wl^4}{EI}\left[.097-.027\right] = \frac{.07\,wl^4}{EI}$$

For $w = w_\Delta l = .0132$ #/in

$l = 11.06$ in

$E = 9.8 \times 10^6$ psi } (of P6)

$I = .019$ in^4

$$\Delta_{\substack{\text{TRIAN.}\\\text{LOAD}}} = \frac{(.07)(.0132)(11.06)^4}{(9.8\times10^6)(.019)} = 74.3 \times 10^{-6}\ \text{in}$$

$$\Delta_{TOTAL} = \Delta_{UNIF} + \Delta_{TRIA} = (39.2 + 74.3)\,10^{-6} = 113.5 \times 10^{-6}\ \text{in}$$

@ 6328 Å, $\lambda = 25 \times 10^{-6}$ in

$\therefore \Delta_{TOTAL} = 4.5\lambda$

NOTE - THIS IS AN IMPROVEMENT OF ~ 1λ (20%) OVER THE "UNIFORM DISTRIBUTION" MODEL; BUT IS STILL LARGER THAN THE JPL SOLUTION BY ABOUT A FACTOR OF 4. THIS DISCREPANCY IS DUE MAINLY TO THE INABILITY OF THE "TAPERED - CANTILEVER BEAM" MODEL EMPLOYED TO ACCOUNT FOR THE HOOP (TANGENTIAL) STIFFNESS INHERENT IN THE MIRROR. THE CONCLUSION CAN BE DRAWN THAT THE "TAPERED-BEAM" MODEL APPROACH IS A

BY.....DATE..... SUBJECT..... SHEET NO. 11 OF 57

CHKD. BY.....DATE..... JOB NO.

REASONABLE DESIGN AID IN SIZING LIGHTWEIGHT MIRRORS IN THAT IT PROVIDES RESULTS OF THE CORRECT ORDER OF MAGNITUDE; ALTHOUGH NOT AS PRECISE AS A FINITE-ELEMENT COMPUTER PROGRAM.

SUMMARY OF RESULTS

SELF WEIGHT DEFLECTION

26" MUSHROOM MIRRORS

SOLUTION TYPE	DEFLECTION
JPL-COMPUTER MODEL	1λ
CLOSED FORM TAPERED-BEAM MODEL-UNIFORM WEIGHT DISTRIBUTION	5.6λ
CLOSED FORM TAPERED-BEAM MODEL-SUPERIMPOSED UNIFORM AND TRIANGULAR WEIGHT DISTRIBUTION	4.5λ

$\lambda = 6328\ \text{Å}$

APPENDIX A

ATTACHMENT 2

SELF-WEIGHT DEFLECTION OF A 100 CM (40") DIAMETER MUSHROOM MIRROR THROUGH SCALING LAWS

BY _____ DATE _____ SUBJECT _____ SHEET NO. _____ OF _____

CHKD. BY _____ DATE _____ JOB NO. _____

DETERMINATION OF THE SELF-WEIGHT DEFLECTION OF A 40" DIAMETER MUSHROOM MIRROR

THE SELF-WEIGHT DEFLECTION OF A 40" DIAMETER MUSHROOM MIRROR (SEE FIGURE 1) WILL BE DETERMINED THROUGH THE SCALING UP OF THE SELF-WEIGHT DEFLECTION OF THE 26" DIAMETER "JPL" MUSHROOM MIRROR (SEE FIGURE 2) FOR WHICH A COMPUTER SOLUTION HAS BEEN PERFORMED:

REF- JPL REPORT # 750-7, REV A, "SUMMARY OF THE COMPUTER ANALYSES ON THE PHOTOHELIOGRAPH MIRROR", PAGE 7, TABLE 7, "SUMMARY OF THE COMPUTER ANALYSES ON THE PHOTOHELIOGRAPH MIRROR", RUN # 2 - "1-G LOAD - MIRROR SUPPORT DOWN".

THE ABOVE REFERENCED COMPUTER SOLUTION PREDICTS A MAXIMUM SELF-WEIGHT DEFLECTION OF 22.0×10^{-6} IN FOR THE 26.12" DIAM. MIRROR.

THIS SOLUTION WILL BE EMPLOYED ALONG WITH PLATE SCALING LAWS TO PREDICT THE CORRESPONDING SELF-WEIGHT DEFLECTION OF THE 40" DIAM.

BY_____DATE_____ SUBJECT_____

CHKD. BY_____DATE_____ JOB NO._____

40 INCH DIAMETER MUSHROOM MIRROR

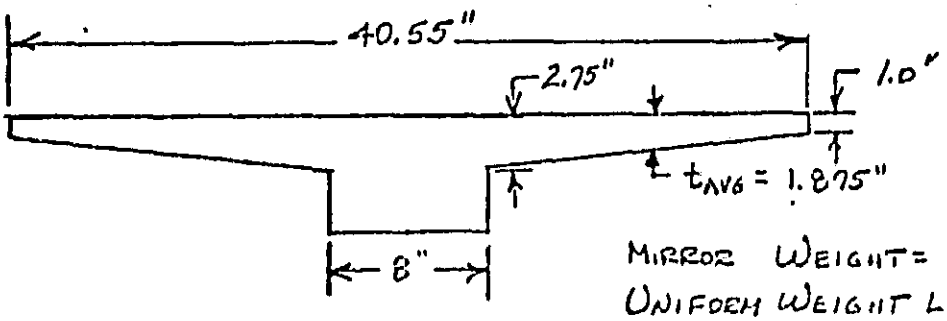

MIRROR WEIGHT = 203 LB.
UNIFORM WEIGHT LOADING =
= 0.161 LB/IN²

FIGURE 1

26 INCH DIAMETER MUSHROOM MIRROR
JPL DESIGN

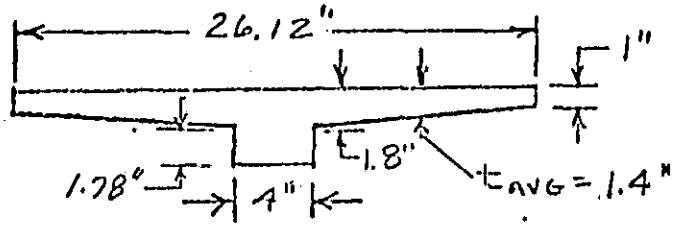

MIRROR WEIGHT = 63 LB (APPROX.)
UNIFORM WEIGHT LOADING = 0.117 LB/IN²

FIGURE 2

BY_____DATE_____ SUBJECT_____ SHEET NO._____OF_____

CHKD. BY_____DATE_____ _____ JOB NO._____

IT IS KNOWN THAT FOR A HUB-MOUNTED MIRROR OF CONSTANT THICKNESS, THE SELF-WEIGHT DEFLECTION IS A COMPLEX FUNCTION OF THE DIAMETER, THE THICKNESS AND THE WEIGHT LOADING. HOWEVER, THE FUNCTION HOLDS THE FOLLOWING APPROXIMATE PROPORTIONALITIES:

$$\Delta \propto \left(\frac{W D^4}{t^3}\right)$$

Where:

W = UNIFORM WEIGHT LOADING

D = MIRROR DIAMETER

t = MIRROR THICKNESS (CONSTANT)

THIS RELATIONSHIP MAY BE USED AS AN APPROXIMATE SCALING RULE FOR DETERMINING THE SELF-WEIGHT DEFLECTION OF THE 40" ϕ MIRROR KNOWING THE SELF-WEIGHT DEFLECTION OF THE 26" ϕ MIRROR, AS FOLLOWS:

$$\Delta_{\substack{40"\phi \\ \text{MIRROR}}} = \Delta_{\substack{26"\phi \\ \text{MIRROR}}} \left[\frac{\left(\frac{W_{40"}}{W_{26"}}\right)\left(\frac{D_{40"}}{D_{26"}}\right)^4}{\left(\frac{t_{40"}}{t_{26"}}\right)^3}\right]$$

BY_____DATE_____ SUBJECT_____ SHEET NO._____OF_____

CHKD. BY_____DATE_____ _____ JOB NO._____

_____ _____ _____

Where: $\Delta_{\substack{26"\phi \\ \text{MIRROR}}}$ = SELF-WEIGHT DEFLECTION = 22×10^{-6} IN (STRESSING)

$W_{40"}$ = UNIFORM WT LOADING = 0.161 #/IN² (cf FIG. 1)

$W_{26"}$ = " " " = 0.117 #/IN² (cf FIG 2)

$D_{40"}$ = DIAMETER = 40.55" (cf FIG 1)

$D_{26"}$ = DIAMETER = 26.12" (cf FIG 2)

$t_{40"}$ = AVERAGE THICKNESS = 1.875" (cf FIG 1)

$t_{26"}$ = " " = 1.4" (cf FIG 2)

WITH THE ABOVE

$$\Delta_{\substack{\text{SELF-WT} \\ 40"\phi \\ \text{MIRROR}}} = (22\times10^{-6})\left[\frac{\left(\frac{0.161}{0.117}\right)\left(\frac{40.55}{26.12}\right)^4}{\left(\frac{1.875}{1.4}\right)^3}\right] = 73.2\times10^{-6}\ \text{IN}$$

@ 6328 Å, $\lambda = 25\times10^{-6}$ IN.

$$\Delta_{\substack{\text{SELF-WT} \\ 40"\phi \\ \text{MIRROR}}} = 2.9\,\lambda$$

THIS RESULT CAN BE COMPARED WITH THE RESULTS OF A "TAPERED-BEAM" APPROACH TO THIS PROBLEM (SEE APPENDIX C) WHICH PREDICTS A SELF-WEIGHT DISTORTION OF 8.8 λ. THE DISCREPANCY BETWEEN THIS RESULT AND THE ABOVE

BY.....DATE..... SUBJECT..... SHEET NO.....OF.....
CHKD. BY.....DATE..... ..... JOB NO. .....
....

CAN BE ATTRIBUTED TO TWO MAIN LIMITATIONS OF THE TAPERED BEAM ANALYSIS EMPLOYED:
A) THE CONSERVATIVE ASSUMPTION OF A UNIFORM WEIGHT DISTRIBUTION EQUAL TO THE MAXIMUM LOCAL WEIGHT THROUGHOUT THE ENTIRE WING AND B) THE INABILITY OF THE BEAM MODEL TO ACCOUNT FOR THE HOOP (TANGENTIAL) STIFFNESS OF THE MIRROR. IN ADDITION, A THIRD FACTOR TO CONSIDER IN THIS COMPARISON IS THAT THE SCALING LAW EMPLOYED IS ONLY APPROXIMATE AND, THEREFORE, ITS RESULTS SHOULD ONLY BE CONSIDERED ON A QUALITATIVE BASIS.

THE IMPORTANT CONCLUSION TO BE DRAWN HERE IS THAT BOTH THE "SCALING" APPROACH AND THE "TAPERED-BEAM" APPROACH ARE APPROXIMATE TECHNIQUES THAT YIELD RESULTS WHICH ARE OF THE SAME ORDER OF MAGNITUDE.

APPENDIX A

ATTACHMENT 3

SELF-WEIGHT DEFLECTION ANALYSIS VIA TAPERED-BEAM METHOD
100 CM (40") DIAMETER MUSHROOM MIRROR

BY _____ DATE _____ SUBJECT _____ SHEET NO. 1 OF 4

CHKD. BY _____ DATE _____ JOB NO. _____

SELF-WEIGHT DEFLECTION

10" DIAM. SOLID TAPER CER-VIT MIRROR

HUB MOUNTED

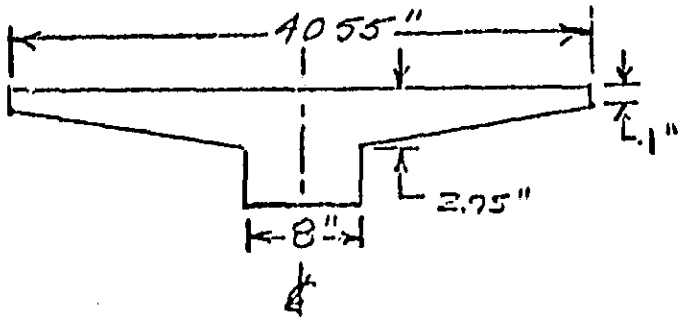

NOTE - IGNORE FRONT AND REAR FACE CURVATURE

WEIGHT = 208 #

FOR ANALYSIS PURPOSES, CONSIDER A 1° RADIAL SEGMENT AS A DOUBLY-TAPERED CANTILEVER BEAM WITH THE CENTRAL HUB AS RIGID.

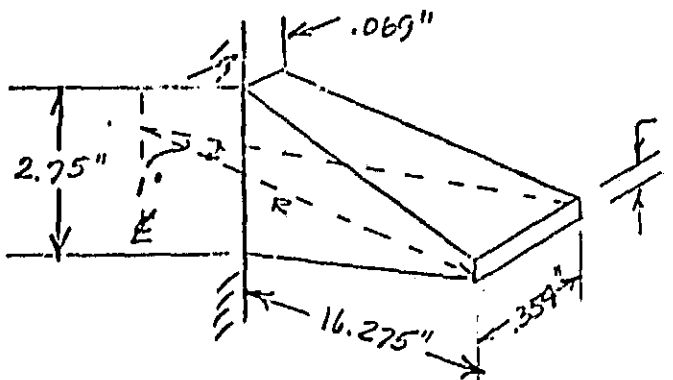

CANTILEVER BEAM MODEL

NOT TO SCALE

BY _____ DATE _____ SUBJECT _____ SHEET NO. 5 OF _____

CHKD. BY _____ DATE _____ JOB NO. _____

CONSIDER THE FOLLOWING BEAM MODEL

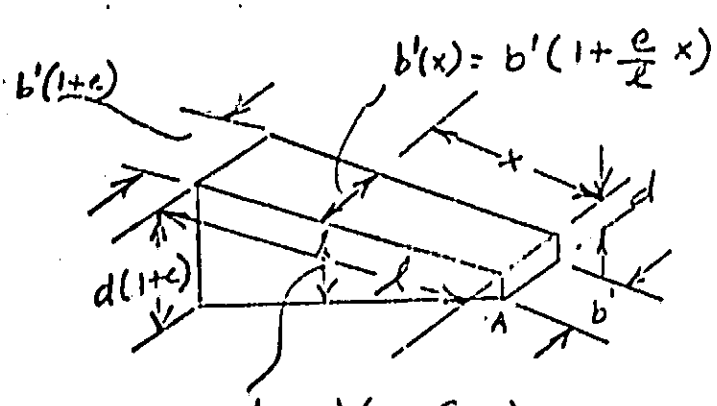

$$I_A = \frac{1}{12} b' d^3 = I$$

$$I_x = I\left(1+\frac{e}{\ell}x\right)\left(1+\frac{c}{\ell}x\right)^3$$

$$A(x) = b'd\left(1+\frac{e}{\ell}x\right)\left(1+\frac{c}{\ell}x\right)$$

FOR SELF WEIGHT LOADING, $W = f(x) = \gamma A(x)$ #/in

CONSERVATIVELY APPLY $W_{MAX} = \gamma A_{MAX}$ TO BEAM AS UNIFORM LOAD.

TO DETERMINE A_{MAX}

$$\frac{dA(x)}{dx} = 0 = \left(\frac{e+c}{\ell}\right) + \frac{2ecx}{\ell^2}$$

$$\boxed{X = -\left(\frac{e+c}{\ell}\right)\left(\frac{\ell^2}{2ec}\right) = -\left(\frac{e+c}{2ec}\right)\ell}$$

TO DETERMINE e, c, ℓ FOR THIS SYSTEM

$$\left.\begin{aligned} b'(1+e) &= 4.0(\theta) \\ b' &= 20.275\,\theta \end{aligned}\right\} \Rightarrow 1+e = \frac{4.0}{20.275},\quad e = -0.802$$

$$\left.\begin{aligned} d(1+c) &= 2.75 \\ d &= 1.0 \end{aligned}\right\} \Rightarrow 1+c = 2.75,\quad c = 1.75$$

BY_____DATE_____ SUBJECT_____ SHEET NO._____OF_____

CHKD. BY_____DATE_____ _____ JOB NO._____

_____ _____ _____

For $\begin{cases} l = 20.275 - 4.0 = 16.275 \\ e = -0.802 \\ c = 1.75 \end{cases}$

$$X = -\left(\frac{e+c}{2ec}\right)l = -\left\{\frac{-.802+1.75}{2(-.802)(1.75)}\right\}\{16.275\} = 5.497$$

$\therefore$ A_{MAX} occurs @ $x = 5.497$"

$$A(5.497) = b'd\left(1+\frac{e}{l}x\right)\left(1+\frac{c}{l}x\right)\Big]_{x=5.497}$$

For $b' = .354$, $d = 1.0$, $e = -.802$, $c = 1.75$, $l = 16.275$"

$$A_{MAX} = (0.354)(1.0)\left[\left(1+\frac{[-.802][5.497]}{16.275}\right)\left(1+\frac{[1.75][5.497]}{16.275}\right)\right]$$

$$A_{MAX} = (0.354)(0.729)(1.591) = 0.41 \text{ in}^2$$

$$W_{MAX} = \rho A_{MAX} = (.08\ \#/\text{in}^3)(0.41) = .0328\ \#/\text{in}$$

→ <u>Apply as uniform load to tapered beam</u>

BY _____ DATE _____ SUBJECT _____ SHEET NO. 1 OF 7

CHKD. BY _____ DATE _____ JOB NO. _____

16- Self Weight Deflection

Considering the 1° radial segment beam with a uniform loading of .0328 #/in (cf P13)

$$\Delta_{MAX\ SELF-WT.} = \left[\frac{wl^4}{2EI}\right]\left[\frac{3c-2e}{c^2(e-c)^2(1+c)} + \frac{2+c}{2c^2(e-c)(1+c)^2} - \frac{1}{e(e-c)^3}\ln(1+c) + \frac{e^2-3c(e-c)}{c^3(e-c)^3}\ln(1+c)\right]$$

where: $I = \frac{1}{12}b'd^3$ (see P. 12)

For: $w = 0.0328$ #/in

$l = 16.275$ in (cf P13)

$E = 9.8\times10^6$ psi

$I = \frac{1}{12}b'd^3 = \left(\frac{1}{12}\right)(0.354)(1.0)^3 = 0.0295$ in.^{4}

$c = 1.75$

$e = -0.802$ } (cf P13)

$$\Delta_{MAX\ SELF-WT} = \left[\frac{(.0328)(16.275)^4}{2(9.8\times10^6)(.0295)}\right]\left[\frac{3(1.75)-2(-.802)}{(1.75)^2(-.802-1.75)^2(1+1.75)} + \frac{2+1.75}{2(1.75)^2(-.802-1.75)(1+1.75)^2} - \frac{1}{(-.802)(-.802-1.75)^3}\ln(1-.802) + \frac{(-.802)^2-3(1.75)(-.802-1.75)}{(1.75)^3(-.802-1.75)^3}\ln(1+1.75)\right]$$

BY _____ DATE _____ SUBJECT _____ SHEET NO. _____ OF _____ 1

CHKD. BY _____ DATE _____ JOB NO. _____

$$\Delta_{MAX}_{SELF-WT} = [3979.949 \times 10^{-6}] [.124961 - .121733 + .12195 +$$

$$- .159462] = 219.976 \times 10^{-6} \text{ in}$$

@ 6328 Å, $\lambda = 25 \times 10^{-6}$ in

$$\Delta_{MAX} = 8.8 \lambda.$$

THIS CAN BE COMPARED WITH THE 2.9λ RESULT OBTAINED BY SCALING UP THE JPL COMPUTER SOLUTION WITH THE DISCREPANCY DUE MAINLY TO THE LIMITATIONS INHERENT IN THE ABOVE "TAPERED-BEAM" APPROACH AS DISCUSSED IN APPENDICES A AND B.

APPENDIX B

SUGGESTED ATD STUDIES
(Solar Telescope)

Based on the recommended primary mirror configuration, the following activities are suggested in support of the ultimate Solar Telescope program. Listed in order of priority, they will assist in preventing program delays incurred by lack of critical technology and assist in selection of optimum subsystem configurations for the application prior to initiation of design effort on these subsystems. Items 1 through 5 may be considered separately or as a set.

1. Stress and Deflection Studies of the Primary

Determine through computer studies the flight stresses, self-weight deflections, and minimum natural frequencies expected for the primary mirror configuration to accurately assess its performance. This information is required for mirror blank selection and specification, overall instrument performance analysis and specification, and preliminary performance tolerance allocation for both Balloon and Orbital Missions.

2. Metrology Mount

Select from among the candidate metrology mount options, that which is best for the candidate mirror configuration and perform computer studies to determine the actual number of support points and their spacings to yield the desired intersupport deformations. Perform preliminary design on the final concept for the candidate mirror configuration to determine the cost.

3. Flight Mount

In connection with #1, consider the 1-G operating environment of the Balloon flight and 0-G orbital environment. Generate flight mount concepts for the mirror configuration, and through computer studies assess the

number of support points, their spacing, their effect on performance and the resulting costs and risk factors. This information is invaluable in estimating ultimate program cost and comparison cost.

4. CTE Variations

Determine the reasonable coefficient of thermal expansion variations expected in the blank for the 65 cm mirror configurations. Perform computer studies to determine the resulting thermal distortions in the mirror under the expected solar, thermal input. Develop the optimum mirror configuration, mounting and resulting thermal control requirements to maintain system performance.

5. Primary Mirror Active Optics

Determine the possible requirements for a back-up active optics system. Through analysis, determine possible operational deformations and subsequently required corrections. Using computer studies, assess the relative difficulty of achieving desired performance for the mirror configuration, the number of required actuators, and range of motions.

6. Secondary Mirror Actuation System

Determine performance requirements of a secondary mirror actuation system for the solar telescope for these requirements. Generate candidate actuation systems and consider their relative performance, cost and risk. Characteristics such as response, range, stability, etc. need be considered for the Solar Telescope Mission and with the specifics of its optical design in mind. This will include performance control and IMC.

7. Thermal Design of The Payload

Do a complete thermal design of the payload to assess the requirements for an active or passive system. Verify the expected thermal inputs and its variations to the primary and secondary mirrors.

8. Primary Mirror Scatter Requirements

Conduct a BRDF analysis of the telescope primary mirror to determine scatter effects on final imagery and develop a meaningful specification for this parameter. The substantial energy incident on the primary mirror combined with the method of field-of-view selection indicates substantial performance impact from this source. Perkin-Elmer developments of analytical methods in this technology area, partially developed under current NASA contract, allow accurate computer analysis.

9. Heat Stop Mirror and Coatings

Determining the performance requirements of the Heat Stop Mirror. With these requirements generate candidate designs and evaluate them for structural thermal and optical performance, cost and risk factors, consider mirror coating requirements, their costs, risks and impact on performance, including light scatter, UV coating degradation, durability and ageing.

Others Include: GREP structure design and analysis
Analysis of the secondary mount

Data Handling

Sensors

Focus and wavefront error sensor

APPENDIX C

MINISCUS MIRRORS

Paragraph 2.4 referred to miniscus mirrors in the discussion of alternate metrology mounts. These mirrors share the same basic, thin tapered outline and mounting arrangement with the mushroom mirror under consideration in this study.

This geometric similarity implies a similarity in all of the considerations inherent in the design and manufacture of primary mirrors of this type.

Perkin-Elmer has successfully designed and fabricated a number of high quality miniscus mirrors up to an aperture of 30 inches with at least $\lambda/4$ figure. Experience includes a 30 inch f/0.62 primary for the Super Schmidt Meteor Camera for NASA and a 26 inch solid miniscus mirror, as well as several of lightweight, sandwich construction.

The differences between these miniscus mirrors and the mushroom mirror lie basically in the mounting arrangements and in the methods of construction. The miniscus mirrors were mounted with hub mounts at their center of gravity as shown in Figure 2 of paragraph 2.4. The construction techniques consisted of front and rear faceplates with a core made of either radial ribs - see Figure 6 - eggcrate construction, or axial cylinders. These differences, however, are only minor and the technology required to build them is directly applicable to the mushroom mirror.

The above experience and its direct applicability to mushroom mirrors is directly applied to the preceding evaluations of mushroom mirror designs for performance and manufacturability.

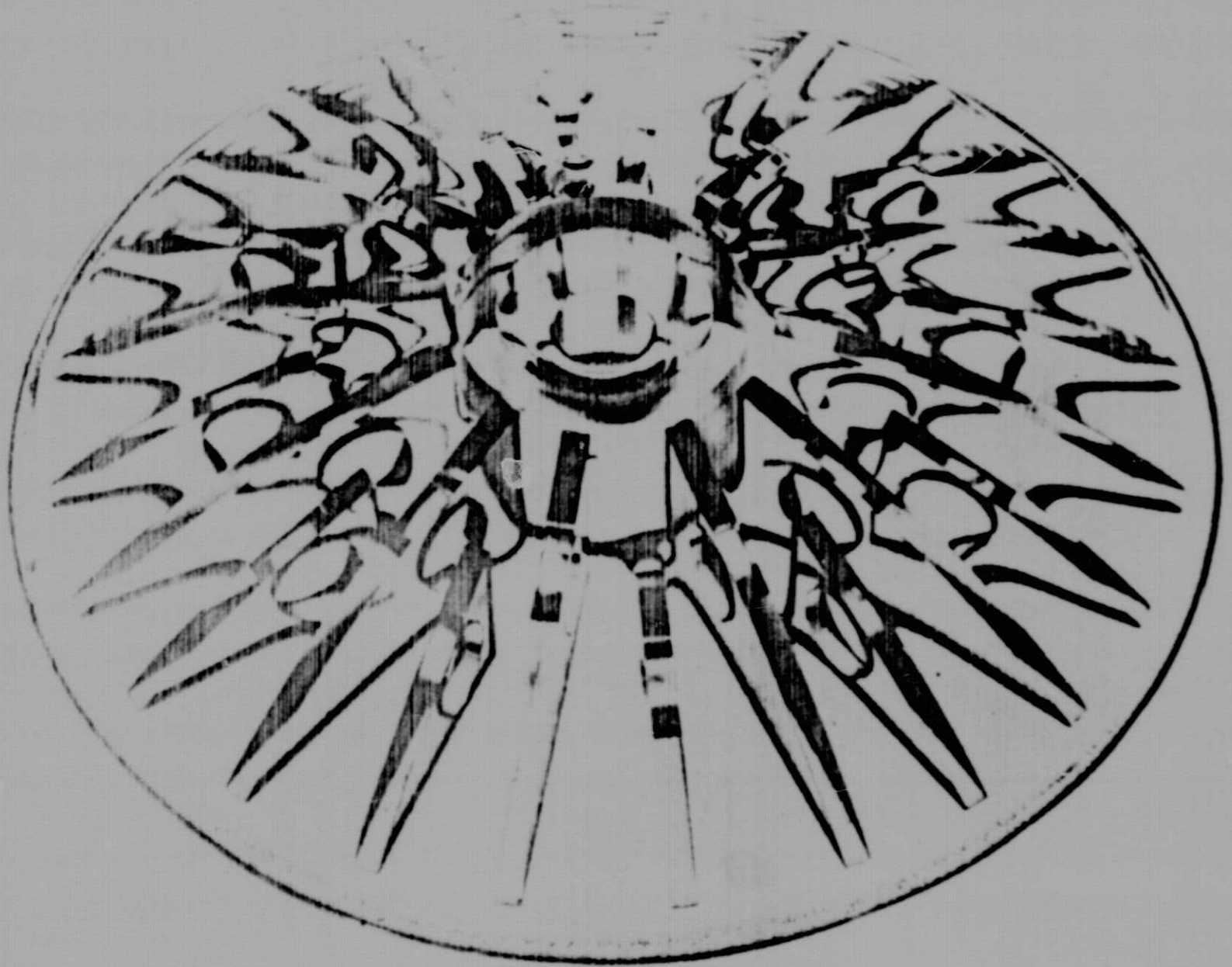

Figure 6.

PERKIN-ELMER - 12" Lightweight Mushroom Mirror